

New Jersey Institute of Technology Digital Commons @ NJIT

Theses

Theses and Dissertations

Spring 1968

Realization of transfer impedances using distributed RC elements in a common ground Linvill configuration

Walter Woronka

New Jersey Institute of Technology

Follow this and additional works at: <https://digitalcommons.njit.edu/theses>

 Part of the [Electrical and Electronics Commons](#)

Recommended Citation

Woronka, Walter, "Realization of transfer impedances using distributed RC elements in a common ground Linvill configuration" (1968). *Theses*. 1493.

<https://digitalcommons.njit.edu/theses/1493>

This Thesis is brought to you for free and open access by the Theses and Dissertations at Digital Commons @ NJIT. It has been accepted for inclusion in Theses by an authorized administrator of Digital Commons @ NJIT. For more information, please contact digitalcommons@njit.edu.

Copyright Warning & Restrictions

The copyright law of the United States (Title 17, United States Code) governs the making of photocopies or other reproductions of copyrighted material.

Under certain conditions specified in the law, libraries and archives are authorized to furnish a photocopy or other reproduction. One of these specified conditions is that the photocopy or reproduction is not to be “used for any purpose other than private study, scholarship, or research.” If a user makes a request for, or later uses, a photocopy or reproduction for purposes in excess of “fair use” that user may be liable for copyright infringement,

This institution reserves the right to refuse to accept a copying order if, in its judgment, fulfillment of the order would involve violation of copyright law.

Please Note: The author retains the copyright while the New Jersey Institute of Technology reserves the right to distribute this thesis or dissertation

Printing note: If you do not wish to print this page, then select “Pages from: first page # to: last page #” on the print dialog screen

The Van Houten library has removed some of the personal information and all signatures from the approval page and biographical sketches of theses and dissertations in order to protect the identity of NJIT graduates and faculty.

REALIZATION OF TRANSFER IMPEDANCES
USING DISTRIBUTED RC ELEMENTS
IN
A COMMON GROUND LINVILL CONFIGURATION
BY
WALTER WORONKA

A THESIS
PRESENTED IN PARTIAL FULFILLMENT OF
THE REQUIREMENTS FOR THE DEGREE
OF
MASTER OF SCIENCE IN ELECTRICAL ENGINEERING
AT
NEWARK COLLEGE OF ENGINEERING

This thesis is to be used only with due regard to the rights of the author. Bibliographical references may be noted, but passages must not be copied without permission of the College and without credit being given in subsequent written or published work.

Newark, New Jersey
1968

APPROVAL OF THESIS
REALIZATION OF TRANSFER IMPEDANCES
USING DISTRIBUTED RC ELEMENTS
IN
A COMMON GROUND LINVILL CONFIGURATION
BY
WALTER WORONKA
FOR
DEPARTMENT OF ELECTRICAL ENGINEERING

BY
FACULTY COMMITTEE

APPROVED: _____

NEWARK, NEW JERSEY

JUNE, 1968

- 1 -

ABSTRACT

One of several synthesis procedures available for the realization of a transfer admittance is that of Linvill. This synthesis procedure employs an active element, a negative impedance converter (NIC), to shift the poles of passive immittance functions from the negative real axis into the complex plane to realize the desired transfer immittance function.

The Linvill synthesis procedure is extended to networks containing cascaded distributed RC elements and the conditions which must be satisfied to realize a transfer impedance using these distributed elements are defined..

72456

ACKNOWLEDGEMENT

I am grateful to Dr. R. W. Wyndrum of Bell Telephone Laboratories for his suggestion of the topic and for his guidance and advice during the development of this thesis. I am especially grateful to Dr. William I. H. Chen of Bell Telephone Laboratories for his careful reading of the manuscript. I also wish to thank William Boynton of International Telephone and Telegraph Laboratories for his computer programing assistance.

TABLE OF CONTENTS

| | |
|--------------|--|
| CHAPTER I. | Introduction of Active Filters |
| 1-1 | Area of Investigation |
| 1-2 | Historical Background |
| CHAPTER II. | Mathematical Characterization of Active \overline{RC} Networks |
| 2-1 | Properties of \overline{URC} Elements |
| 2-1.1 | Basic Characteristics of Distributed \overline{RC} Elements |
| 2-1.2 | Transformation and Mapping |
| 2-2 | Linville's Network Configuration |
| CHAPTER III. | Properties of Active \overline{RC} - NIC Cascaded Networks |
| 3-1 | Characteristics of Transfer Functions Using Cascaded \overline{RC} Networks |
| 3-2 | Realization of Pole Pairs via Linville's Configuration |
| 3-3 | Example of the Linville's \overline{RC} Network Configuration |
| CHAPTER IV. | Conclusion |
| 4-1 | Summary of Results |
| 4-2 | Suggestions for Future Work |
| APPENDIX A | Development of Positive Real Transformation |
| APPENDIX B | Negative Impedance Converter Properties |
| APPENDIX C | Solutions of Second Order Transfer Functions |

CHAPTER I. INTRODUCTION TO ACTIVE FILTERS

1-1 Area of Investigation

Active \overline{RC} filters have become practical, reliable and precise due to the advancing technology of monolithic and thin film integrated circuit development and fabrication. The application of microminiatureization techniques has resulted in lower cost; improvement of system reliability and significant reduction of size. The practicality of active networks is a direct result of the availability of stable resistors and capacitors of small size with compensated temperature coefficients.

Since active elements have become compatible with passive networks, several active network realization procedures for driving point and transfer immittances, and transfer voltage ratios have resulted.¹⁻⁶ The active element employed may be either a negative impedance converter,⁷ a high gain stabilized feedback amplifier or a gyrator. The active element simply is used to shift the poles of passive immittance functions from the negative real axis into the complex plane to realize the desired immittance function. The ability to control the pole and zero locations in the S-plane using an active element permits the design of highly selective

low pass, high pass as well as band pass networks without the use of inductors.

This paper defines the conditions which must be satisfied to realize a transfer impedance via the Linvill network configuration, using cascaded \overline{RC} elements. The specific configuration is shown in Figure 13.

1-2 Historic Background

A uniform distributed RC element^{8,9} is defined as a distributed transmission line having only series resistance and shunt capacitance uniformly distributed per unit length. The distributed \overline{RC} structure is of multi-layer construction with the resistive layer and the capacitive layer separated by a dielectric as shown in Figure 1. In general the \overline{RC} element is constructed such that the length is much greater than the width. The inductance of a typical element is negligible below 100 KHz.

In 1963, significant progress in the area of exact network synthesis of distributed RC networks was made by Wyndrum⁸. The synthesis procedure utilizes a positive real mapping technique which transforms the transcendental expressions characterized by a distributed element into the simpler, non-transcendental form or finite polynomials. This transformation results in lumped LC functions growing out of the original RC functions, permitting the use of network theory¹⁰⁻¹³ developed specifically for lumped LC functions. Wyndrum¹⁴ shows that the repeated use of Richard's theorem¹⁴ to extract unit RC sections from a desired impedance function results in the realization of the desired transfer or driving point function by a cascade of a finite number of RC sections.

A method for the realization of transmission zeros was presented using a stub as a zero preparation element followed by extraction of other RC elements to complete the realization of the desired transmission zeros.

9

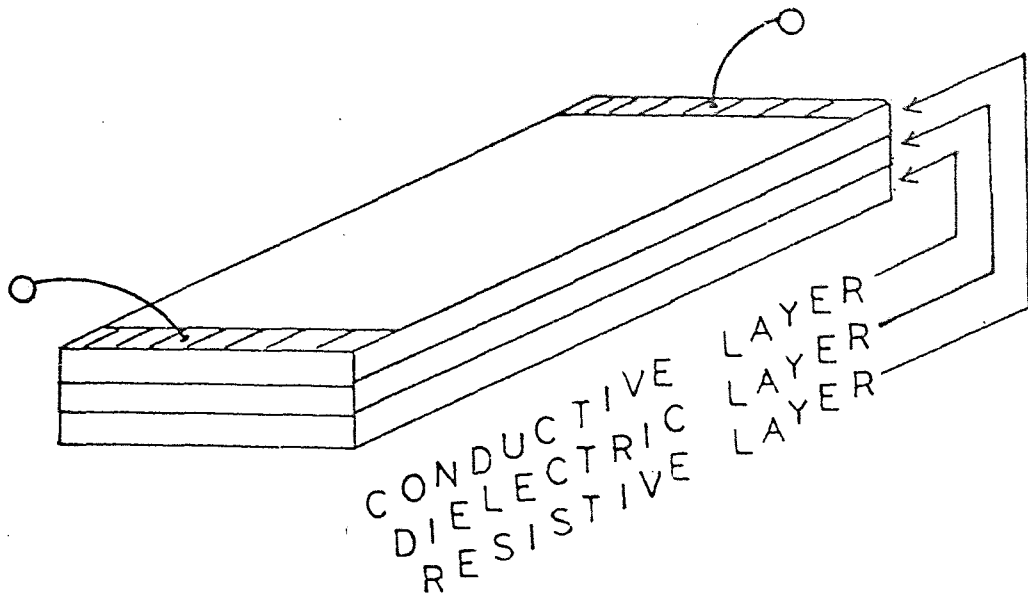
In 1965, O'Shea presented a synthesis procedure for driving point and transfer functions using an equivalent transformation technique. The synthesis procedure for the driving point impedance was identical in capabilities to that presented by Wyndrum, but did not necessarily result in a common ground network.

Work in the area of passive distributed network synthesis progressed with the cascade synthesis of distributed networks presented by Scanlan and Rhodes¹⁵. Their development used the transformation presented by Wyndrum and is restricted to functions which may be realized by a cascade of two-port RC sections, series or short-circuited stubs, and shunt open-circuited stubs leading to rational functions after transformation. Another restriction imposed was that the network elements all had commensurate length, i.e. $RC = \sqrt{\tau}$ or multiples thereof for each section. Necessary conditions for realization of any short circuit or open circuit immittance parameters together with the sufficiency condition for simultaneous realization of any two such

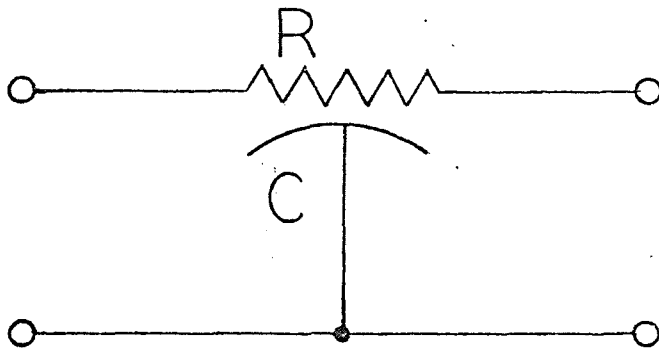
parameters have been formulated.

16

In 1966, Stein, Mulligan, and Shamis developed the necessary and sufficient conditions for the realization of open-circuit \overline{URC} voltage transfer functions. The synthesis is in the form of commensurate length having a common ground connection. The cascade network is composed of realization cycles containing a "zero preparation" element followed by an RC element and finally followed by a series or shunt stub to realize the transmission zero. An extraction technique using Richard's theorem was used to realize the transmission zeros of the desired function. The authors used the transformation presented by Wondrum with an additional step of transforming from the lumped LC plane to the lumped RC plane.



PHYSICAL STRUCTURE



SYMBOLIC REPRESENTATION

FIGURE 1

CHAPTER II. MATHEMATICAL CHARACTERIZATION OF ACTIVE
RC NETWORKS

2-1 Properties of \overline{URC} Elements

2-1.1 Basic Characteristics. A uniform \overline{RC} line open circuited segment, shown in Figure 2, is characterized by the ABCD parameters⁸

$$\begin{vmatrix} A & B \\ C & D \end{vmatrix} = \begin{vmatrix} \cosh \sqrt{RCs} & \frac{R \sinh \sqrt{RCs}}{\sqrt{RCs}} \\ \frac{\sqrt{RCs} \sinh \sqrt{RCs}}{R} & \cosh \sqrt{RCs} \end{vmatrix} \quad (2-1)$$

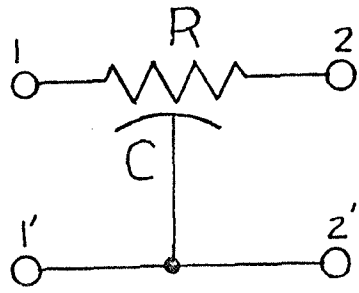
where R and C are in ohms per unit length and farads per unit length respectively. The equivalent Z-parameters for the single \overline{RC} segment are

$$\begin{vmatrix} Z_{11} & Z_{12} \\ Z_{21} & Z_{22} \end{vmatrix} = \begin{vmatrix} \frac{R \coth \sqrt{RCs}}{\sqrt{RCs}} & \frac{R \operatorname{csch} \sqrt{RCs}}{\sqrt{RCs}} \\ \frac{R \operatorname{csch} \sqrt{RCs}}{\sqrt{RCs}} & \frac{R \coth \sqrt{RCs}}{\sqrt{RCs}} \end{vmatrix} \quad (2-2)$$

The expression for the transfer impedance for a single open-circuited \overline{RC} element is given by

$$Z_{21}(s) = \frac{R \operatorname{csch} \sqrt{RCs}}{\sqrt{RCs}} \quad (2-3)$$

and is characterized by a pole at the origin followed by an infinite number of discrete poles in the S-plane positioned on the negative real axis.



$$Z_{11} = \frac{R \coth \sqrt{RC} S}{\sqrt{RC} S}$$

 \Rightarrow

$$\frac{R \coth \sqrt{RC} S}{\sqrt{RC}}$$

 \Rightarrow

$$\frac{\infty}{W}$$

$$Z_{21} = \frac{R \operatorname{csch} \sqrt{RC} S}{\sqrt{RC} S}$$

 \Rightarrow

$$\frac{R \operatorname{csch} \sqrt{RC} S}{\sqrt{RC}}$$

 \Rightarrow

$$\frac{\infty}{W(1-W^2)^{1/2}}$$

S-PLANE
(\overline{RC} PLANE)

$$Z_{\overline{RC}}(S)$$

\sqrt{S} PLANE
(\overline{LC} PLANE)

$$Z_{\overline{LC}}(\sqrt{S})$$

W PLANE
(LC PLANE)

$$Z_{LC}(W)$$

FIGURE 2

The pole locations of Z_{21} are located at

$$s = - \frac{\pi^2 n^2}{\tau} \quad (2-4)$$

where $\tau = RC$ and $n = 0, 1, 2, \dots, \infty$

A transmission zero is located at infinity.

Since a single open-circuited uniform \overline{RC} element is both bilateral and symmetrical, the roots of Z_{12} and Z_{21} are identical. The open circuit driving point impedances are given by

$$Z_{11} = Z_{22} = \frac{R \coth \sqrt{\tau s}}{\sqrt{\tau s}} \quad (2-5)$$

The poles of the driving point impedances are located at

$$s = - \frac{\pi^2 n^2}{\tau} \quad n = 0, 1, 2, \dots, \infty \quad (2-6)$$

and the zeros are located at

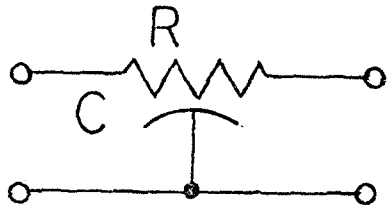
$$s = - \frac{(n + \frac{1}{2})^2 \pi^2}{\tau} \quad n = 0, 1, 2, \dots, \infty \quad (2-7)$$

in the S -plane respectively, as shown in Figure 3.

The poles of the driving point and transfer impedances are negative real in the S -plane.

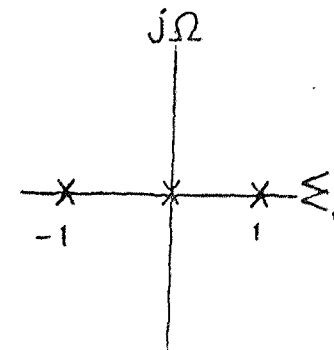
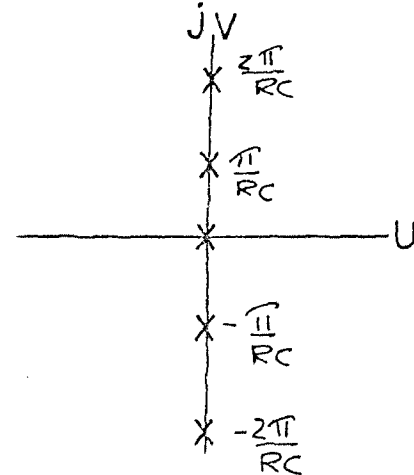
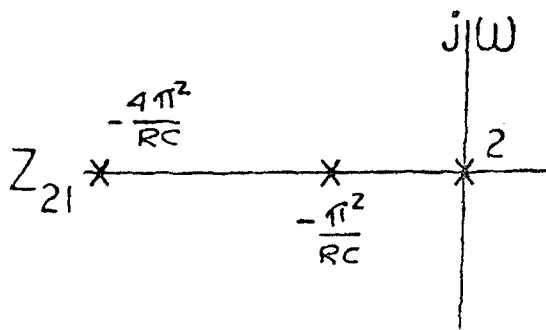
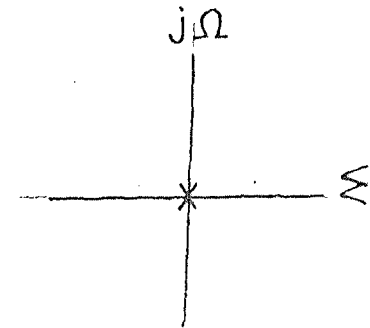
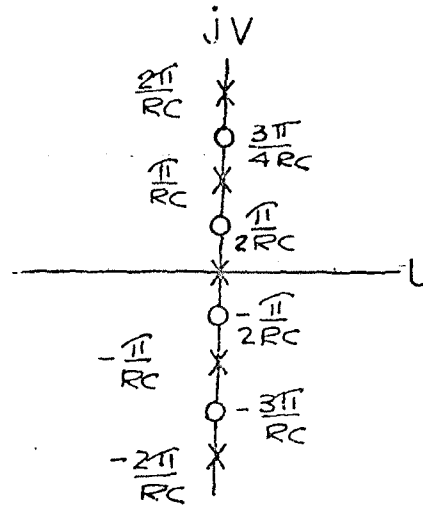
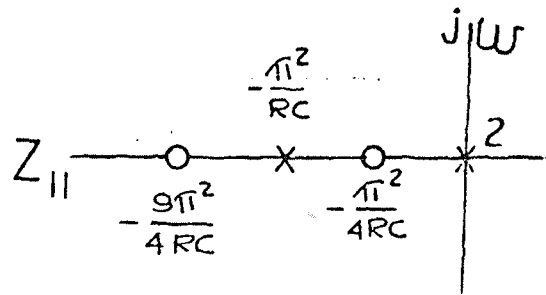
Consider the case when two \overline{RC} elements of the same time constant are cascaded as shown in Figure 4. The ABCD parameters for this case are given by

$$\begin{vmatrix} \cosh^2 \sqrt{\tau s} + \frac{R_1}{R_2} \sinh^2 \sqrt{\tau s} & \frac{(R_1 + R_2) \cosh \sqrt{\tau s} \sinh \sqrt{\tau s}}{\sqrt{\tau s}} \\ \frac{R_1 R_2 \sqrt{\tau s} \cosh \sqrt{\tau s} \sinh \sqrt{\tau s}}{(R_1 + R_2)} & \cosh^2 \sqrt{\tau s} + \frac{R_2}{R_1} \sinh^2 \sqrt{\tau s} \end{vmatrix} \quad (2-8)$$



$$Z_{11}(s) = \frac{R \coth \sqrt{RCs}}{\sqrt{RCs}}$$

$$Z_{21}(s) = \frac{R \operatorname{csch} \sqrt{RCs}}{\sqrt{RCs}}$$



S-PLANE

S-PLANE
FIGURE 3

W-PLANE

The driving point impedance using (2-8) is given by

$$Z_{11} = \frac{(R_1 + R_2) \left[\cosh^2 \sqrt{\tau s} + \frac{R_1}{R_2} \sinh^2 \sqrt{\tau s} \right]}{R_1 R_2 \sqrt{\tau s} \cosh \sqrt{\tau s} \sinh \sqrt{\tau s}} \quad (2-9)$$

The zeros of Z_{11} are the roots of

$$\tanh^2 \sqrt{\tau s} + \frac{R_2}{R_1} = 0 \quad (2-10)$$

where (2-10) is equivalent to equation (8) in Appendix C. The solution given by (19) and (21) in Appendix C in terms of the constants under consideration here are given by

$$s_1 = -\frac{1}{4\tau} \left[2\pi r_1 - 2 \tan^{-1} \sqrt{\frac{R_2}{R_1}} \right]^2_{r_1=0,1,2,\dots} \quad (2-11)$$

and

$$s_2 = -\frac{1}{4\tau} \left[\pi r_2 - 2 \tan^{-1} \sqrt{\frac{R_2}{R_1}} \right]^2_{r_2=1,2,\dots} \quad (2-12)$$

A transmission zero at infinity arises from the term $\frac{1}{\sqrt{\tau s}}$

The poles of Z_{11} are the roots of the equation

$$\sqrt{\tau s} \cosh \sqrt{\tau s} \sinh \sqrt{\tau s} = 0 \quad (2-13)$$

The poles are located on the negative real axis in the s -plane at the locations given by

$$\left. \begin{aligned} s &= 0 \\ &= -\frac{\pi^2 n^2}{\tau} \\ &= -\frac{(\pi + \frac{1}{2})^2 \pi^2}{\tau} \end{aligned} \right\} n=0,1,2,\dots \quad (2-14)$$

The transfer impedance Z_{Z1_T} for an open circuited two section \overline{RC} element connected in cascade is given by

$$Z_{Z1_T} = \frac{R_1 + R_2}{R_1 R_2 \sqrt{\tau s} \cosh \sqrt{\tau s} \sinh \sqrt{\tau s}} \quad (2-15)$$

with subsequent pole locations in the S-plane

$$\left. \begin{aligned} \text{given by } S &= - \frac{(n + \frac{1}{2})^2 \pi^2}{\tau} \\ &= - \frac{\pi^2 n^2}{\tau} \end{aligned} \right\} n=0, 1, 2, \dots \quad (2-16)$$

Associated with (2-15) is also a transmission zero at infinity.

In general, \overline{RC} elements in cascade do not produce any complex poles. All the singularities of the driving point impedance and the transfer impedance lie on the negative real axis in the S-plane.

2-1.2 Transformation and Mapping. Distributed elements, being characterized by hyperbolic functions, provide an infinite number of distinct poles and zeros in the S-plane immittances. Due to the large number of singularities in the immittance functions, they become difficult to handle, in order to conceptually visualize the frequency response and shape of the functions under consideration. Fortunately, it is possible to conformally map these transcendental functions into other complex planes where the original functions themselves become simpler, being represented by rational polynomials of a new variable.

The first transformation ¹² carries the distributed \overline{RC} plane expressions to the distributed LC plane

$$Z_{LC}(\sqrt{s}) = \sqrt{s} Z_{\overline{RC}}(s) \quad (2-17)$$

Proceeding conversely, from the distributed LC plane to the distributed \overline{RC} plane

$$Z_{\overline{RC}}(s) = \frac{Z_{LC}(\sqrt{s})}{\sqrt{s}} \quad (2-18)$$

The transformation given by (2-17) still contains infinitely many poles and/or zeros in the immittance functions but these singularities are shifted from the negative real axis in the

S-plane to the positive and negative imaginary axis in the \sqrt{S} plane; they remain equally spaced. An additional transformation⁸

$$W = \tanh \sqrt{S}$$

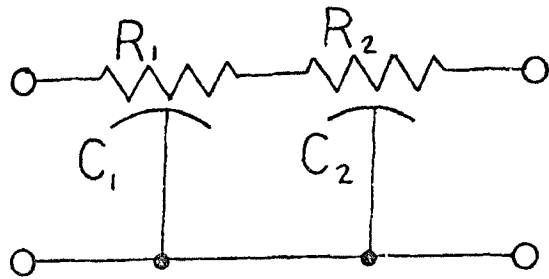
is required to provide functions that may be realized in terms of finite polynomials. This transformation results in lumped LC functions in the W-plane which may be analyzed using network theory developed specifically for lumped elements. The S-plane to W-plane transformation of Z_{11} and Z_{21} parameters for two distributed RC elements in cascade is shown in Figure 4.

It is necessary to become familiar with the $S \rightarrow \sqrt{S} \rightarrow W$ transformation and the mechanics by which the infinite number of poles and zeros become finite terms in the W-plane. The relationship of the W-plane coordinates $W = \Sigma_1 + j\Omega_1$, in terms of the \sqrt{S} plane coordinates are developed in Appendix A via equations (6) and (7) and are given below

$$\Sigma_1 = \frac{\sinh \sqrt{E} U \cosh \sqrt{E} U}{\cos^2 \sqrt{E} V + \sinh^2 \sqrt{E} U} \quad (2-19)$$

$$\Omega_1 = \frac{\sin \sqrt{E} V \cos \sqrt{E} U}{\cos^2 \sqrt{E} V + \sinh^2 \sqrt{E} U} \quad (2-20)$$

In Figure 5, various regions are identified in



$$Z_{II} = \frac{1 + \frac{R_1}{R_2} \text{TANH}^2(R_1 R_2)}{\sqrt{TS} \text{TANH} \sqrt{TS} (R_1 + R_2)}$$

$$Z_{II} = \frac{1 + \frac{R_1}{R_2} \text{TANH}^2 \sqrt{TS} (R_1 R_2)}{\sqrt{T} \text{TANH} \sqrt{TS} (R_1 + R_2)}$$

$$Z_{II} = \frac{1 + \frac{R_1}{R_2} W^2 (R_1 R_2)}{W \sqrt{T} (R_1 + R_2)}$$

$$Z_{2I} = \frac{R_1 R_2}{\sqrt{TS} (R_1 + R_2) \text{COSH} \sqrt{TS} \text{SINH} \sqrt{TS}}$$

$$Z_{2I} = \frac{R_1 R_2}{\sqrt{T} (R_1 + R_2) \text{COSH} \sqrt{TS} \text{SINH} \sqrt{TS}}$$

$$Z_{II} = \frac{(1 - W^2) R_1 R_2}{W \sqrt{T} (R_1 + R_2)}$$

S-PLANE
(RC PLANE)

$$Z_{RC}(s)$$

\sqrt{S} -PLANE
(LC PLANE)

$$Z_{LC}(\sqrt{S})$$

W-PLANE
(LC PLANE)

$$Z_{LC}(w)$$

FIGURE 4

IDENTIFICATION OF CORRESPONDING REGIONS

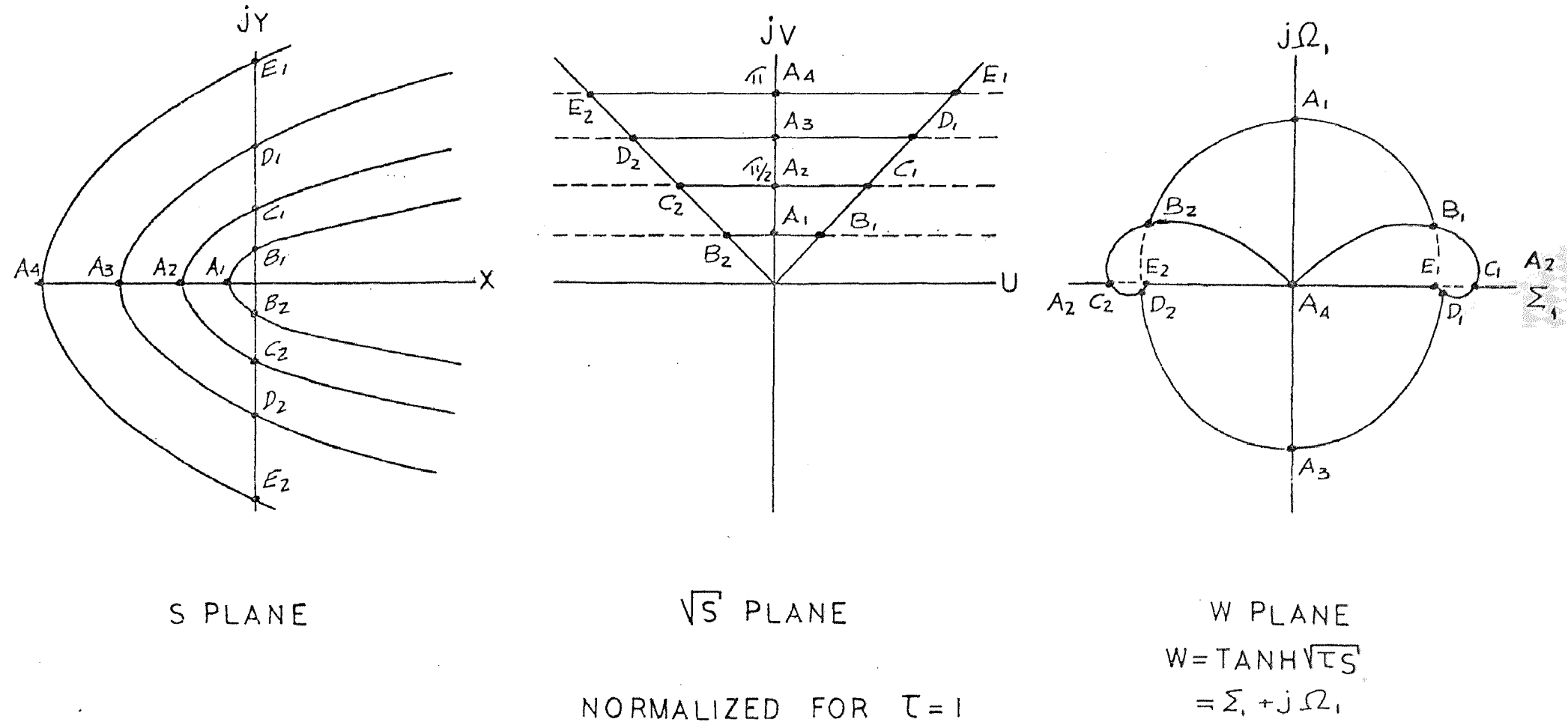


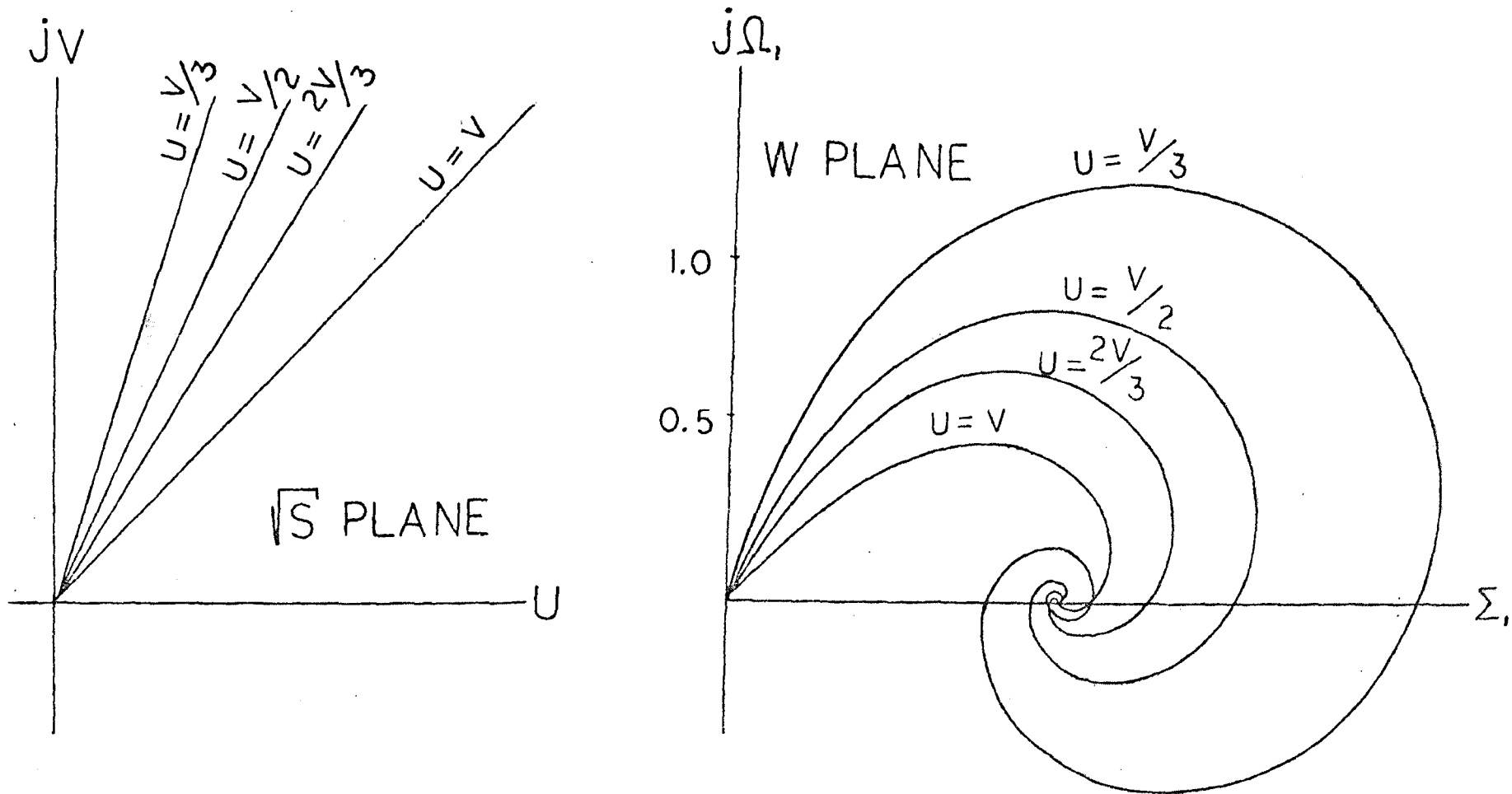
FIGURE 5

$S \rightarrow \sqrt{S} \rightarrow W$ planes respectively. The mapping from $S \rightarrow \sqrt{S}$ plane is not conformal since, although the mapping is on a one to one basis, the angular relationships are not preserved. The $\sqrt{S} \rightarrow W$ plane mapping, however, is conformal. Figure 6 shows the several locus points which are mapped from the S -plane into the W -plane. Since the W -plane plot converges rapidly around $\sum, = /$ (as shown in Figure 6), an expanded area about $\sum, = /$ is shown in Figure 7.

The semi-infinite strip in the \sqrt{S} -plane bounded by the parallel lines $V=0$ and $V=\frac{\pi}{\sqrt{L}}$ map entirely into the W -plane. A strip twice the width, $V=\frac{2\pi}{\sqrt{L}}$, maps into the W -plane twice, once every interval $\frac{\pi}{\sqrt{L}}$. Using a normalizing constant \sqrt{L} in Figure 8, together with Figure 9, the S -plane to W -plane transformations of the semi-infinite strips of width $\frac{\pi}{\sqrt{L}}$ are shown in Figure 10.

The information presented in Figure 6 is expanded and presented on a more accurate scale and shown in Figure 10. Using this enlarged figure, certain boundary limitations are observed.

$U=V$, which is the real frequency contour in the S -plane, is also the boundary of



MAPPING OF LOCUS OF POINTS IN THE
 \sqrt{S} PLANE TO THE W PLANE

FIGURE 6

EXPANDED REAL FREQUENCY
CONTOUR FOR THE VICINITY $\Sigma_1 = 1$

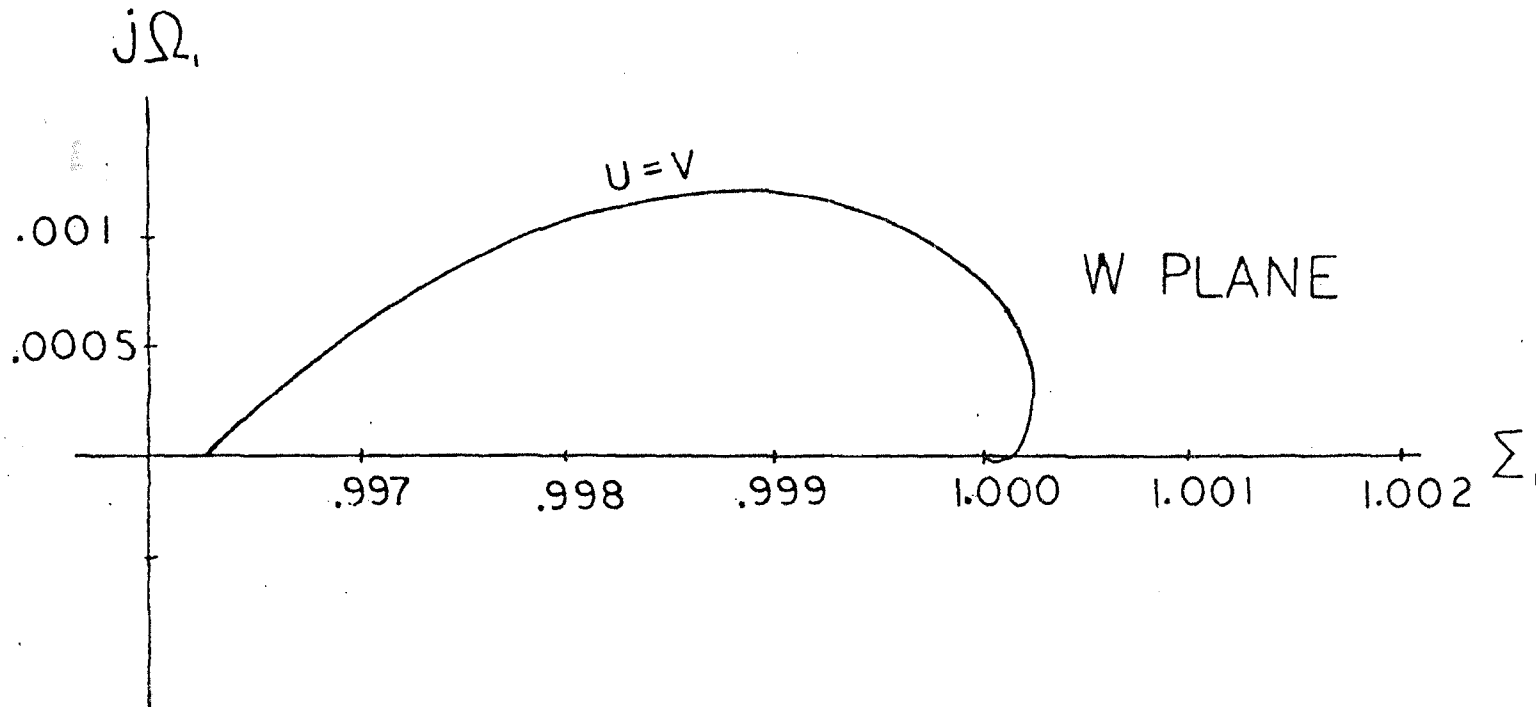
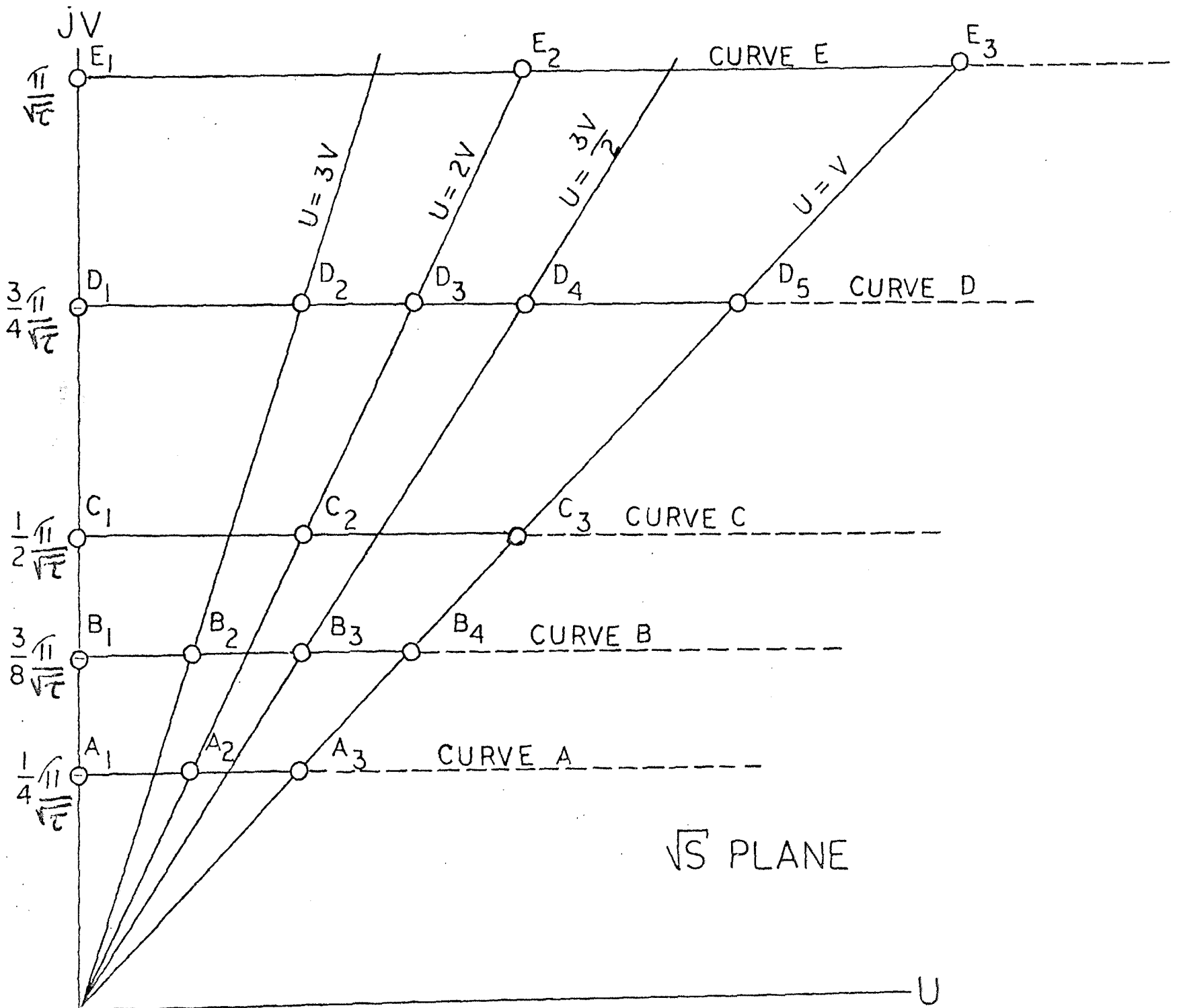


FIGURE 7

FIGURE 8



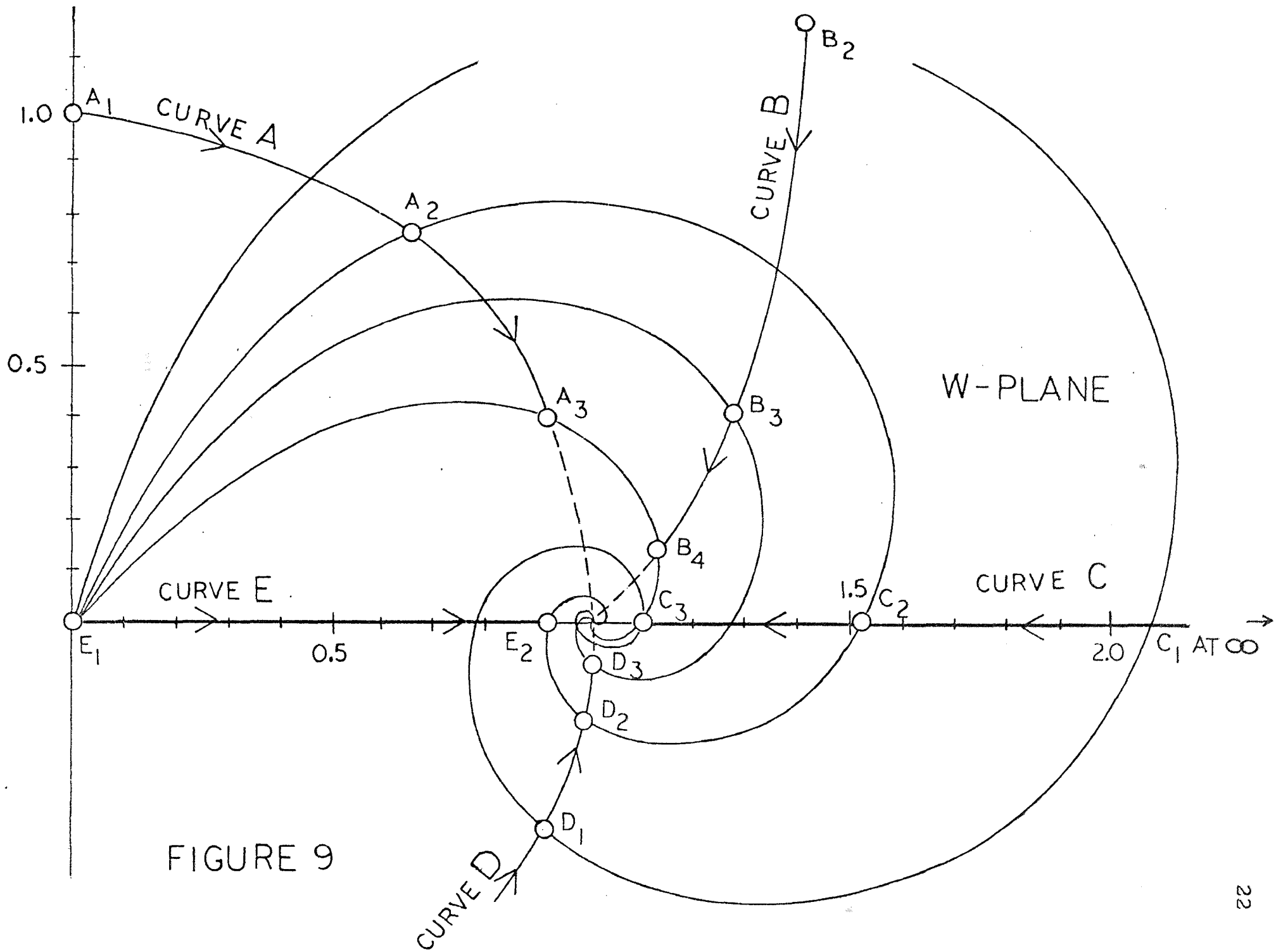
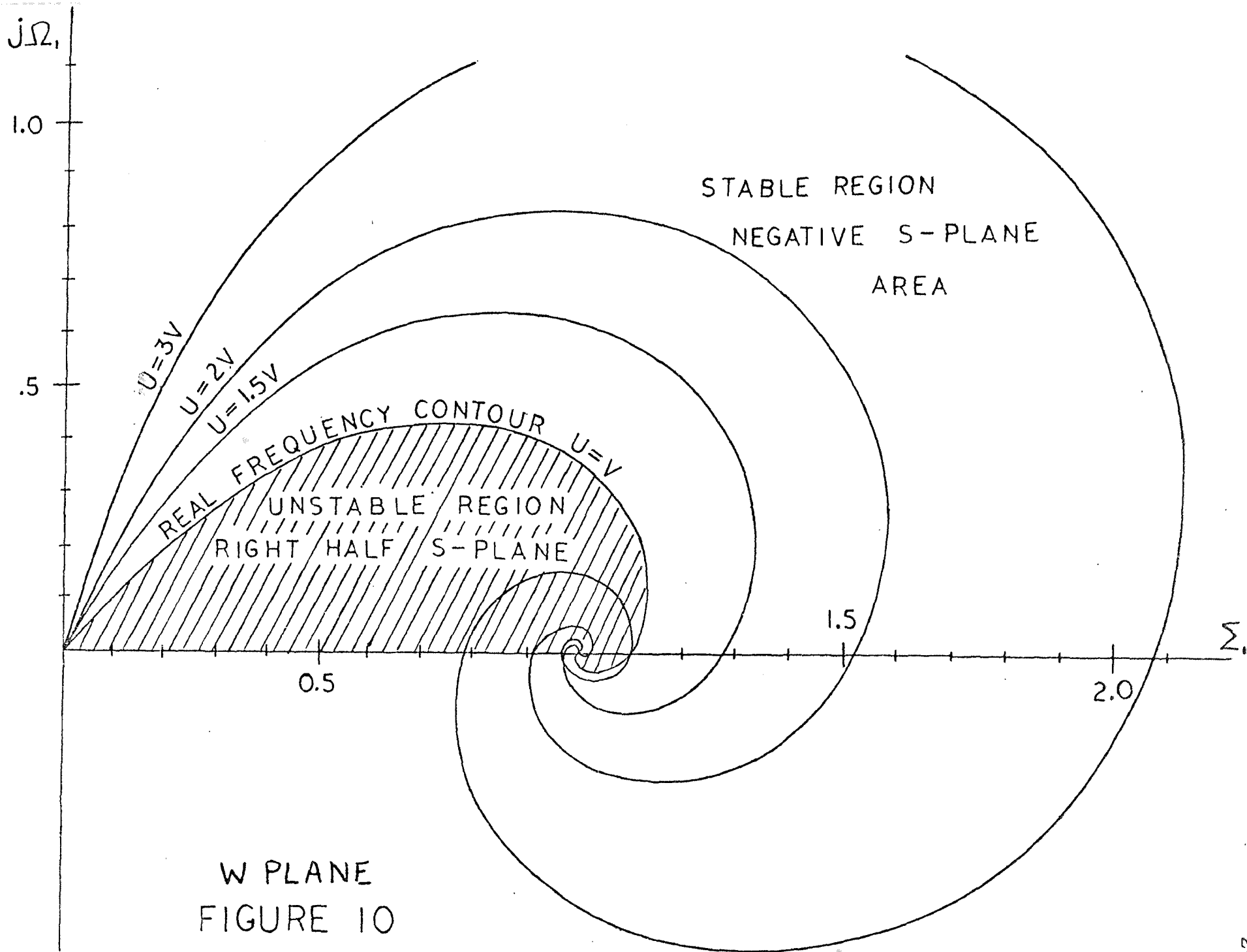


FIGURE 9

the negative real axis. Any response realization performed in the W -plane which has poles within the region bounded by the curve $U=V$ and the line extending from $\Sigma_1=0$ to $\Sigma_1=1$ is therefore unstable. Figure 10 shows the boundary limits between stable and unstable regions.

Since the \sqrt{S} -plane and the W -plane are symmetrical about their imaginary axis, Figures 6 through Figures 10 consider only symmetrical half-planes. The remaining half-planes may be visualized to be mirror image figures presented about the $j\Omega_1$ axis.



2-2 Linville Configuration Network

The Linville configuration is composed of two passive networks interconnected in cascade by a negative impedance converter (NIC) as shown in Figure 11. The general expression for the transfer function using the Linville configuration may be developed by multiplying the ABCD matrices of each passive and active section while preserving the order of multiplication. Using the ABCD parameters of a current inversion negative impedance converter developed in Appendix B and a general matrix for both network N_A and N_B , the overall ABCD network parameters are determined as

$$\begin{vmatrix} A & B \\ C & D \end{vmatrix} = \begin{vmatrix} A_1 & B_1 \\ C_1 & D_1 \end{vmatrix} \begin{vmatrix} K_1 & 0 \\ 0 & -\frac{K_1}{K_2} \end{vmatrix} \begin{vmatrix} A_2 & B_2 \\ C_2 & D_2 \end{vmatrix} \quad (2-21)$$

The result of multiplying (2-21) is the overall matrix for the cascaded configuration

$$\begin{vmatrix} A & B \\ C & D \end{vmatrix}_{\text{TOTAL}} = \begin{vmatrix} \left[K_1 A_1 A_2 - \frac{K_1}{K_2} B_1 C_2 \right] & \left[K_1 A_1 B_2 - \frac{K_1}{K_2} B_1 D_2 \right] \\ \left[K_1 C_1 A_2 - \frac{K_1}{K_2} D_1 C_2 \right] & \left[K_1 C_1 B_2 - \frac{K_1}{K_2} D_1 D_2 \right] \end{vmatrix} \quad (2-22)$$

Since interest is focused on the transfer function for the Linville configuration, only the ABCD to Z-parameter transformation shall be performed to obtain the transfer function!

LINVILL'S NETWORK CONFIGURATION

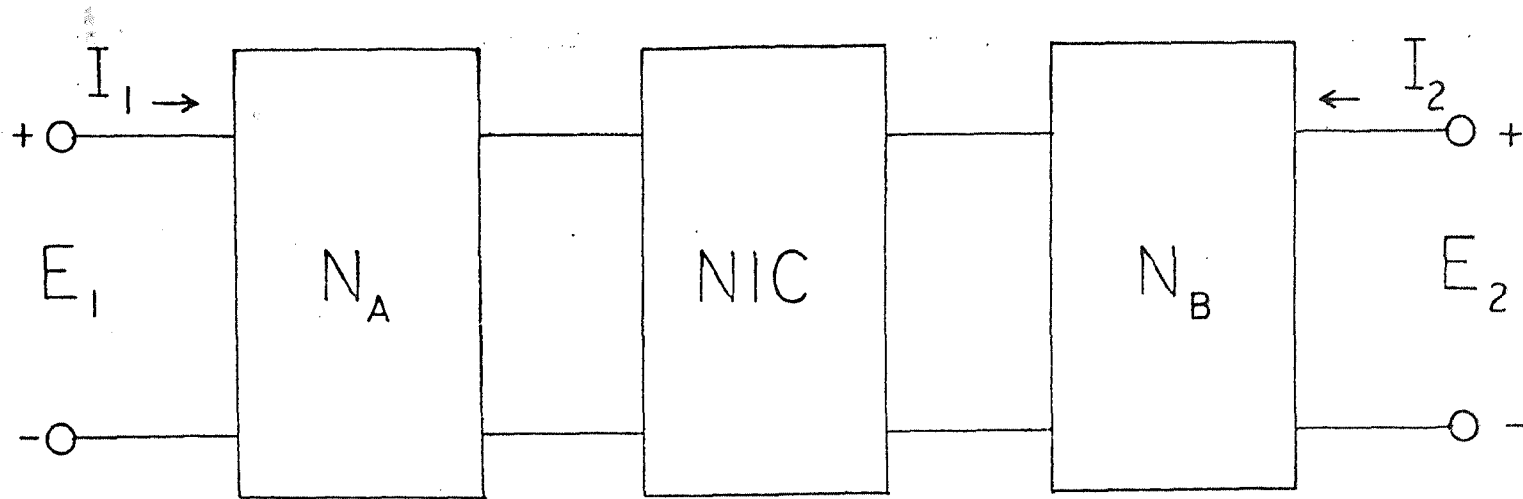


FIGURE II

$$Z_{2IT} = \frac{1}{C_{TOTAL}} \quad (2-23)$$

The expression for the transfer function via (2-22) becomes,

$$Z_{2IT} = \frac{1}{K_1 C_1 A_2 - \frac{K_1}{K_2} D_1 C_2} \quad (2-24)$$

but

$$C_1 = \frac{1}{Z_{21}^{(A)}} \quad (2-25a)$$

$$C_2 = \frac{1}{Z_{21}^{(B)}} \quad (2-25b)$$

$$A_2 = \frac{Z_{11}^{(B)}}{Z_{12}^{(B)}} \quad (2-25c)$$

$$D_1 = \frac{Z_{22}^{(A)}}{Z_{21}^{(A)}} \quad (2-25d)$$

Replacing $Z_{12}^{(B)}$ in (2-25c) with $Z_{21}^{(B)}$ since the passive network is reciprocal and inserting back into (2-24) yields

$$Z_{2IT} = \frac{-\frac{K_2}{K_1} Z_{21}^{(A)} Z_{21}^{(B)}}{Z_{22}^{(A)} - K_2 Z_{11}^{(B)}} \quad (2-26)$$

If $K_2 = K$, then (2-26) becomes

$$Z_{2IT} = \frac{M Z_{21}^{(A)} Z_{21}^{(B)}}{Z_{22}^{(A)} - K Z_{11}^{(B)}} \quad (2-27)$$

where

$$M = -\frac{K_2}{K_1} \text{ INIC} \quad (2-28a)$$

$$M = \frac{K_2}{K_1} \text{ VNIC} \quad (2-28b)$$

CHAPTER III. PROPERTIES OF ACTIVE RC-NIC CASCADED NETWORKS

3-1 Characteristics of Transfer Functions in Cascaded RC Networks

The general expression for the transfer impedance of a Linvill network configuration was developed in section 2-2 equation (2-26) and is given again ^{1,12}

$$Z_{21T} = \frac{\left(\pm \frac{K_2}{K_1}\right) Z_{21}^{(A)} Z_{21}^{(B)}}{Z_{22}^{(A)} - K_2 Z_{11}^{(B)}} \quad (3-1)$$

This expression holds for any general network N_A and N_B . Identifying the networks N_A and N_B as distributed RC elements, consider the case of networks composed of single \overline{RC} sections being identified as N_A and N_B shown in Figure 12. Holding the restriction $R_1^{(A)} C_1^{(A)} = R_1^{(B)} C_1^{(B)} = \tau$ remain constant, the Linvill transfer impedance using single RC elements is developed below.

The W-plane transfer and driving point impedances of a unit \overline{RC} element are given below

$$Z_{11} = Z_{22} = \frac{R_1}{\sqrt{\tau} W} \quad (3-2)$$

$$Z_{21} = \frac{R_1}{\sqrt{\tau}} \frac{\sqrt{1-W^2}}{W} \quad (3-3)$$

Inserting these terms into equation (3-1) yields

$$Z_{21T}(W) = \frac{\left(\pm \frac{K_1}{K_2}\right) R_1^{(A)} R_1^{(B)} (1-W^2)}{\sqrt{\tau} [R_1^{(A)} - K_2 R_1^{(B)}] W} \quad (3-4)$$

LINVILL'S CONFIGURATION FOR REALIZATION
OF TRANSFER IMMITTANCES USING \overline{RC}

ELEMENTS

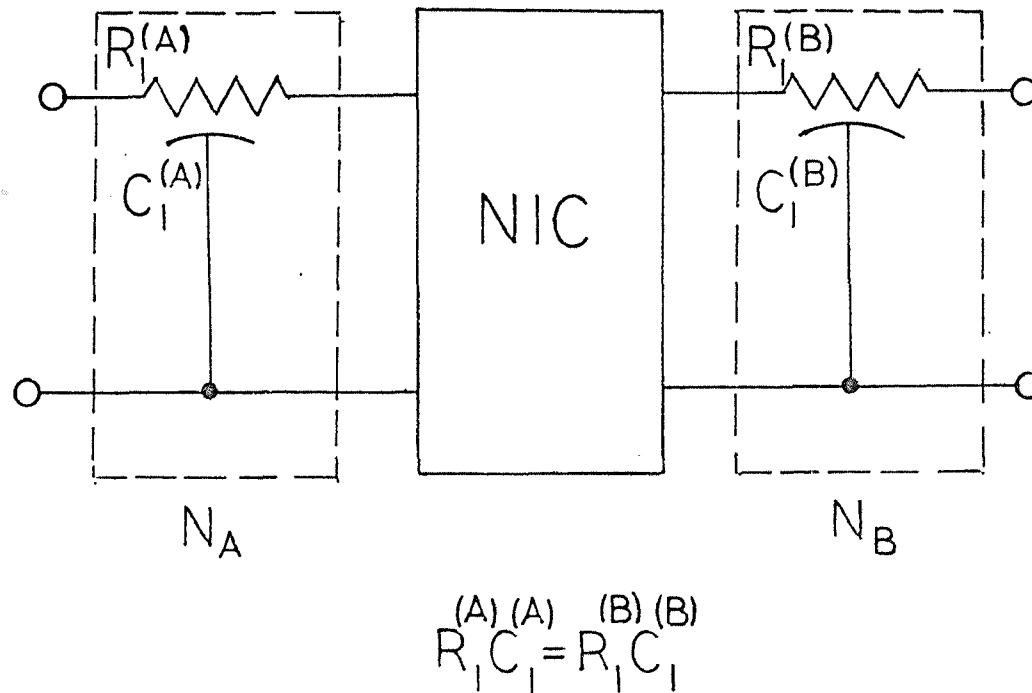
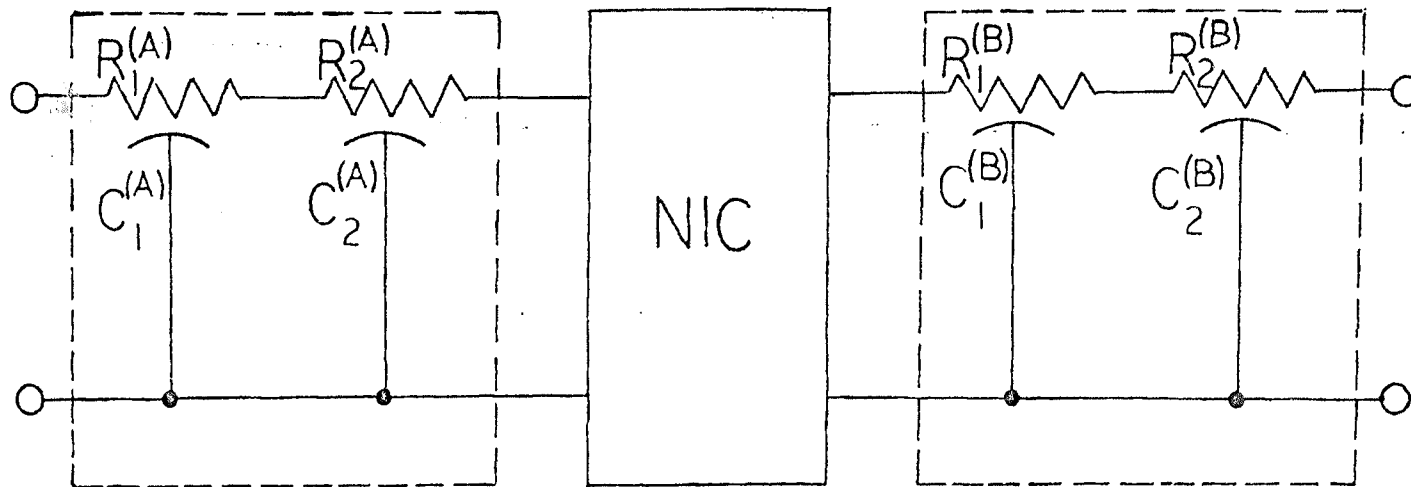


FIGURE 12

LINVILL'S CONFIGURATION FOR REALIZATION OF TRANSFER IMMITTANCES USING \overline{RC}

ELEMENTS



$$N_A \quad R_1^{(B)} C_1^{(B)} = R_1^{(A)} C_1^{(A)} = R_2^{(A)} C_2^{(A)} = R_2^{(B)} C_2^{(B)} \quad N_B$$

FIGURE 13

The transfer function given by (3-4) has the following singularities:

- a) A W-plane pole at the origin which maps into an infinite number of interlaced poles in the S-plane.
- b) Two W-plane zeros at $\sum_i = \pm 1$ which correspond to transmission zeros at infinity in the S-plane.

Consider now the cascade of two \overline{RC} elements in cascade contained within N_A and similarly in N_B . This cascaded \overline{RC} - NIC - \overline{RC} configuration is shown in Figure 13. The required expressions for the two \overline{RC} elements in cascade are given below

$$Z_{11}^{(B)} = \frac{1 + \frac{R_1^{(B)}}{R_2^{(B)}} W^2}{W \left[\frac{\sqrt{L}}{R_1^{(B)}} + \frac{\sqrt{L}}{R_2^{(B)}} \right]} \quad (3-5a)$$

$$Z_{21}^{(A)} = \frac{(1 - W^2)}{W \left[\frac{\sqrt{L}}{R_1^{(A)}} + \frac{\sqrt{L}}{R_2^{(A)}} \right]} \quad (3-5b)$$

$$Z_{21}^{(B)} = \frac{(1 - W^2)}{W \left[\frac{\sqrt{L}}{R_1^{(B)}} + \frac{\sqrt{L}}{R_2^{(B)}} \right]} \quad (3-5c)$$

$$Z_{22}^{(A)} = \frac{1 + \frac{R_2^{(A)}}{R_1^{(A)}} W^2}{W \left[\frac{\sqrt{L}}{R_1^{(A)}} + \frac{\sqrt{L}}{R_2^{(A)}} \right]} \quad (3-5d)$$

Inserting the immittance expressions into (3-1) yields

$$Z_{2IT}(W) = \frac{\left(\pm \frac{K_1}{K_2}\right) [1-W^2]^2}{W \left[1 + \frac{R_2^{(A)}}{R_1^{(A)}} W^2 \right] \left[\frac{\sqrt{L}}{R_1^{(B)}} + \frac{\sqrt{L}}{R_2^{(B)}} \right] - K_2 W \left[1 + \frac{R_1^{(B)}}{R_2^{(B)}} W^2 \right] \left[\frac{\sqrt{L}}{R_1^{(A)}} + \frac{\sqrt{L}}{R_2^{(A)}} \right]} \quad (3-6)$$

Using the following substitutions in (3-6)

$$\beta_1^{(A)} = \frac{R_2^{(A)}}{R_1^{(A)}} \quad (3-7a)$$

$$\beta_1^{(B)} = \frac{R_1^{(B)}}{R_2^{(B)}} \quad (3-7b)$$

$$K^{(A)} = \frac{\sqrt{L}}{R_1^{(A)}} + \frac{\sqrt{L}}{R_2^{(A)}} \quad (3-7c)$$

$$K^{(B)} = \frac{\sqrt{L}}{R_1^{(B)}} + \frac{\sqrt{L}}{R_2^{(B)}} \quad (3-7d)$$

results in a simplification of (3-6) after slight manipulation

$$Z_{2IT}(W) = \frac{\left(\pm \frac{K_2}{K_1}\right) (1-W^2)^2}{W \left[\beta_1^{(A)} K^{(B)} - K_2 \beta_1^{(B)} K^{(A)} \right] \left[\frac{K^{(B)} - K_2 K^{(A)}}{\beta_1^{(A)} K^{(B)} - K_2 \beta_1^{(B)} K^{(A)}} + W^2 \right]} \quad (3-8)$$

In general (3-8) may be written as

$$Z_{2IT}(W) = \frac{M(1-W^2)^2}{W [W^2 \pm Q^2]} \quad (3-9)$$

where

$$M = \frac{\left(\pm \frac{K_2}{K_1}\right)}{\beta_1^{(A)} K^{(B)} - K_2 \beta_1^{(B)} K^{(A)}} \quad (3-10)$$

and

$$Q = \frac{K^{(A)}}{\beta_1^{(B)} K^{(A)}} \sqrt{\frac{\frac{K^{(B)}}{K^{(A)}} - K_2}{\frac{\beta_1^{(A)} K^{(B)}}{\beta_1^{(B)} K^{(A)}} - K_2}} \quad (3-11)$$

are real constants.

In equation (3-11), Q may be either positive or negative depending on the sign of K_2 , the negative impedance conversion ratio, and due to the difference term, the magnitude of K_2 will also alter the sign of (3-11). It is for this reason that the numerator in (3-9) contains the \pm term.

The S-plane pole solutions to (3-9) are derived in Appendix C. For the case when the W-plane transfer impedance is of the form

$$Z_{2IT}(W) = \frac{M(1-W^2)^2}{W(W^2 + Q_1^2)} \quad (3-12)$$

This corresponds to the S-plane transfer impedance given by

$$Z_{2IT}(\sqrt{S}) = \frac{M}{\sinh \sqrt{TS} \cosh^3 \sqrt{TS} (\tanh^2 \sqrt{TS} + Q_1^2)} \quad (3-13)$$

the singularities of which are located at points

$$S = -\frac{(n+\frac{1}{2})^2 \pi^2}{T}, \quad n=0,1,2,\dots \quad (3-14a)$$

$$S = -\frac{n^2 \pi^2}{T}, \quad n=0,1,2,\dots \quad (3-14b)$$

$$S = -\frac{1}{4\tau} \left[2\pi r_1 + 2 \tan^{-1} \theta_1 \right]^2, \quad \begin{array}{l} r_1 = 0, 1, 2, \dots \\ n = 0, 1, 2, \dots \end{array} \quad (3-14c)$$

$$S = -\frac{1}{4\tau} \left[\pi r_2 + 2 \tan^{-1} \theta_1 \right]^2 \quad \begin{array}{l} r_2 = 1, 2, \dots \\ n = 0, 1, 2, \dots \end{array} \quad (3-14d)$$

where the poles given by (3-14a) are third order poles.

From equation (3-14) we see that no complex S-plane pole solutions exist, therefore this selection of circuit constants which provide positive Q

i.e. $\left[\frac{\frac{K^{(B)}}{K^{(A)}} - K_2}{\frac{\beta_1^{(A)} K^{(B)}}{\beta_1^{(B)} K^{(A)}} - K_2} \right]^{\frac{1}{2}}$ is positive do not permit

shaping of the transfer function by manipulating pole positions since all the poles are restricted to the negative real S-plane axis.

A more interesting case exists when Q is negative, under this condition the W-plane transfer function given by (3-12) becomes

$$Z_{2IT}(W) = \frac{M}{W(W^2 - Q_2^2)} \quad (3-15)$$

The corresponding \sqrt{S} -plane transfer function is given by

$$Z_{2IT}(\sqrt{S}) = \frac{M}{\sinh \sqrt{\tau S} \cosh^3 \sqrt{\tau S} (\tanh^2 - \theta_2^2)} \quad (3-16)$$

for which the S-plane pole solutions are

$$S = -\frac{(m + \frac{1}{2})^2 \pi^2}{\tau} \quad m = 0, 1, 2, \dots \quad (3-17a)$$

$$S = -\frac{n^2 \pi^2}{\tau} \quad n = 0, 1, 2, \dots \quad (3-17b)$$

$$S = \frac{1}{4\tau} \left[-\log_e \left| \frac{1-Q_2}{1+Q_2} \right| + j \left(\pi \lceil r_3 + 1 \rceil - \Phi \right) \right]^2 \quad \begin{matrix} r_3 = 1, 2, \dots \\ \Phi = \kappa \pi \\ \kappa = 0, 1, 2, \dots \end{matrix} \quad (3-17c)$$

$$S = \frac{1}{4\tau} \left[-\log_e \left| \frac{1+Q_2}{1-Q_2} \right| - j \left(\pi \lceil r_4 \rceil - \Phi \right) \right]^2 \quad \begin{matrix} r_4 = 0, 1, 2, \dots \\ \Phi = \kappa \pi \\ \kappa = 0, 1, 2, \dots \end{matrix} \quad (3-17d)$$

The S-plane solutions of (3-17) do provide complex pole pairs in the transfer function.

3-2 Realization of Pole Pairs via Linvill Configuration

The Linvill network configuration for realization of transfer impedances using cascaded \overline{RC} elements can provide the following W-plane pole roots:

- a) Zeros of higher order at the points $\Sigma = \pm 1$ depending upon the number of cascaded sections under consideration.
- b) A pole at the origin, independent of the number of sections under consideration.
- c) A conjugate pair of poles either on the imaginary W-plane axis or the real W-plane axis due to the difference term in the denominator of the transfer impedance.

Due to the network configuration, one of two possible cases may evolve:

- a) $\beta_1^{(B)}$ is greater than $\beta_1^{(A)}$ (ref. equation (3-7) sec. 3-1). Under this condition when the NIC conversion ratio K_2 is zero, the roots lie at points $A \notin A'$, see Figure 14. As the conversion ratio K_2 approaches $\frac{\beta_1^{(A)} K^{(B)}}{\beta_1^{(B)} K^{(A)}}$ the poles approach \pm infinity, along the imaginary W-plane axis. When $\frac{\beta_1^{(A)} K^{(B)}}{\beta_1^{(B)} K^{(A)}} K_2 < \frac{K^{(B)}}{K^{(A)}}$ the poles lie on the real axis and are at the origin when $K_2 = \frac{K^{(B)}}{K^{(A)}}$. For $K_2 > \frac{K^{(B)}}{K^{(A)}}$ the poles are on the imaginary axis and approach $B \notin B'$ in the limit.

POLE PAIR LOCATIONS FOR LINVILL'S SYNTHESIS USING CASCADED \overline{RC} SECTIONS

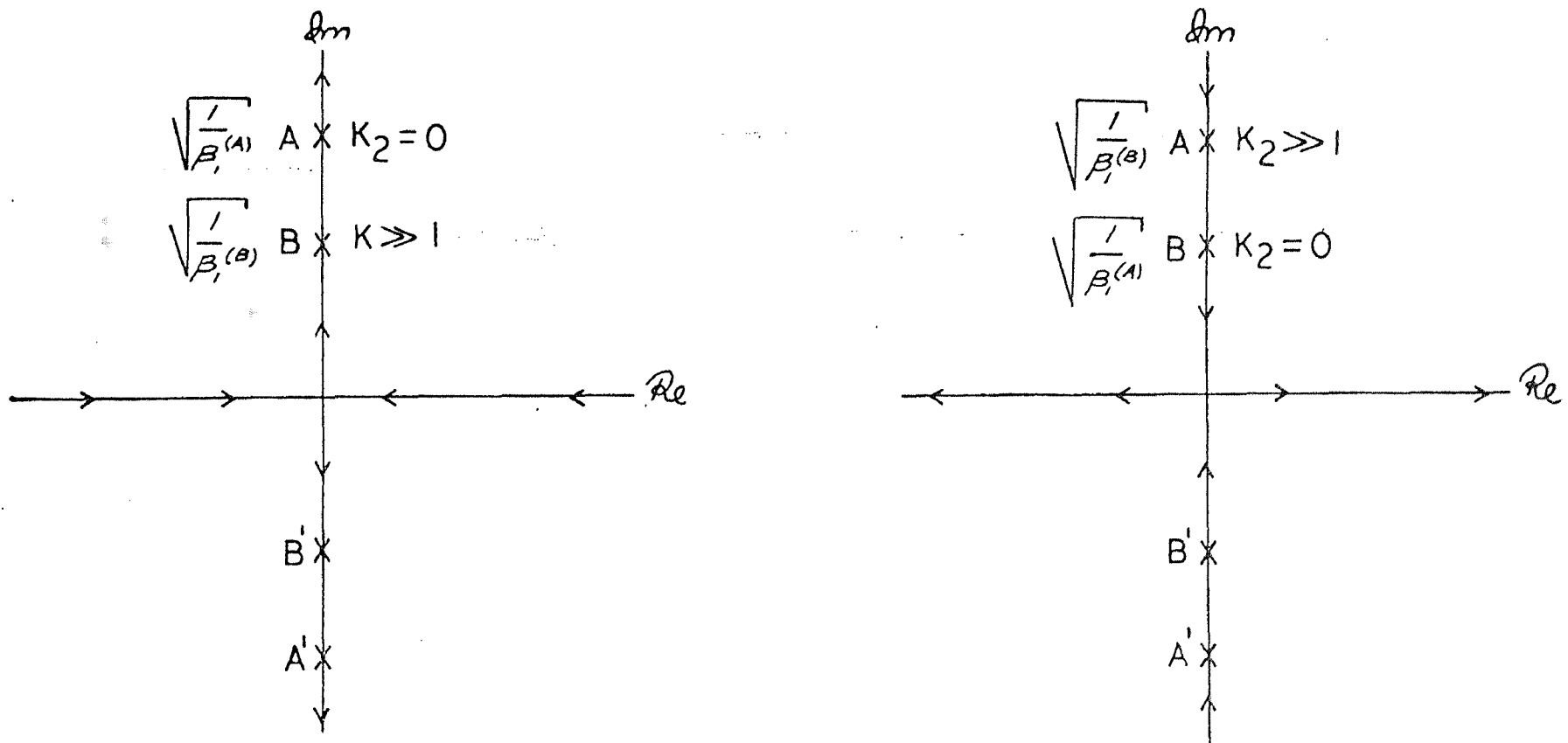


FIGURE 14

b) $\beta_1^{(A)}$ is greater than $\beta_1^{(B)}$. Under this condition when the NIC conversion ratio K_2 is zero, the poles lie at $B \& B'$, see Figure 14. As the conversion ratio K_2 approaches $\frac{K^{(B)}}{K^{(A)}}$ the poles approach the origin. When $\frac{K^{(B)}}{K^{(A)}} < K_2 < \frac{\beta_1^{(A)} K^{(B)}}{\beta_1^{(B)} K^{(A)}}$ the poles lie on the positive and negative real W-plane axis and approach infinity as $K_2 \rightarrow \frac{\beta_1^{(A)} K^{(B)}}{\beta_1^{(B)} K^{(A)}}$. For $K_2 > \frac{\beta_1^{(A)} K^{(B)}}{\beta_1^{(B)} K^{(A)}}$, the poles appear on the imaginary axis and approach the points $A \& A'$ as K_2 gets very large.

The case when the W-plane pole locations lie on the imaginary axis corresponds to the negative real axis S-plane poles and is of no interest since shaping of the transfer impedance is not possible.

When the W-plane pole locations exist on the real axis, complex S-plane pole solutions are obtained. Precaution should be taken since RH S-pole solutions are also possible.

THEOREM I. A sufficient condition for the realization of a transfer impedance with complex poles using cascaded \overline{RC} elements in a Linvill configuration is that the W-plane poles lie on the real axis at points not less than 1.0903.

THEOREM II. A transfer function with S-plane poles in the LHP can be realized using cascaded \overline{RC} elements in a Linvill configuration.

3-3 Example of the Linvill RC Network Configuration

Consider the example shown in Figure 15. The time constant for the network is $\tau = 3$. Using the values given in Figure 15 and substituting into equation (3-7) section 3-1 yields

$$\beta_1^{(A)} = 0.468 \quad (3-18a)$$

$$\beta_1^{(B)} = 29.2 \quad (3-18b)$$

$$K^{(A)} = 0.936 \quad (3-18c)$$

$$K^{(B)} = 12.51 \quad (3-18d)$$

inserting these values into equation (3-8) section 3-1 yields

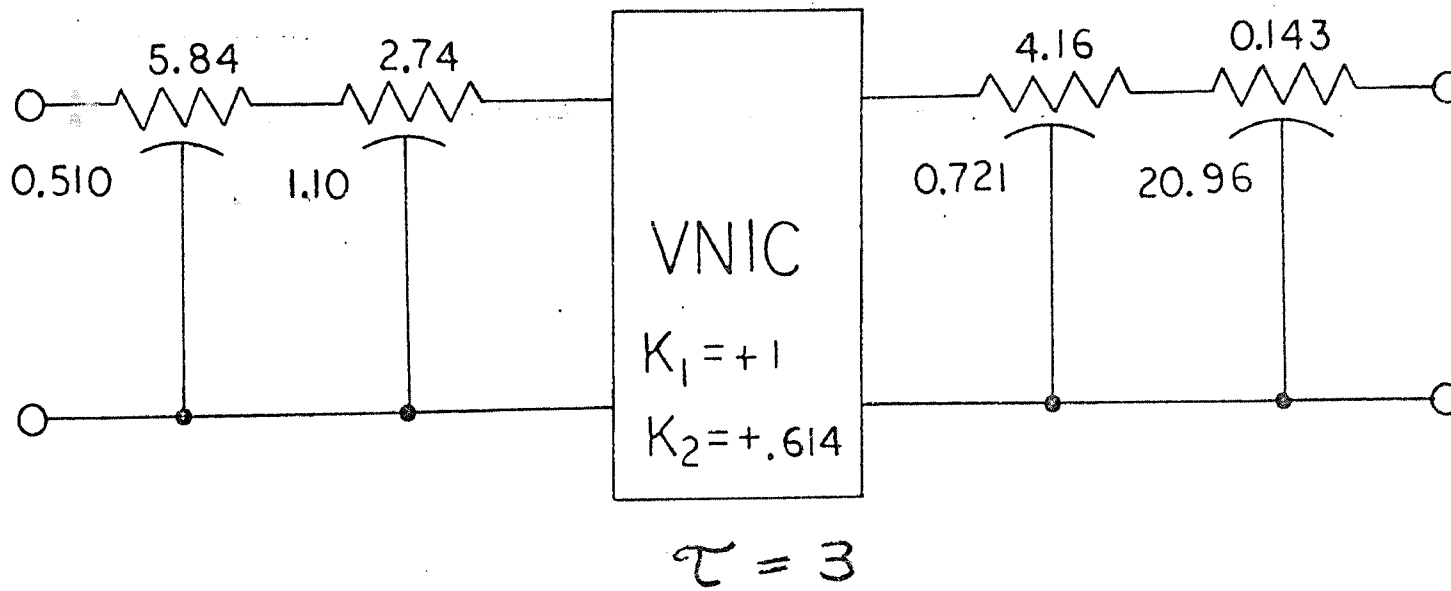
$$Z_{21T}(w) = \left(-\frac{K_2}{K_1}\right) \left(\frac{1}{5.82 - 27.3K_2}\right) \left[\frac{(1 - w^2)^2}{w \left[w^2 + \left(\sqrt{\frac{12.51 - 0.936K_2}{5.82 - 27.3K_2}} \right)^2 \right]} \right] \quad (3-19)$$

Using Figure 10, it is seen that the real frequency contour intersects the w -plane real axis at $\Sigma = \pm 1.0903$ which represents the boundary between the region of stability and instability. Poles on the real w -plane axis located at points less than $\Sigma = 1.0903$ correspond to poles in the RH s -plane.

The value of K_2 which provides the value for $\Sigma = \sqrt{1.0903}$ is found to be $K_2 = 0.614$. Choose $K_1 = 1$; then the total expression becomes

$$Z_{21T}(w) = \frac{0.056(1 - w^2)^2}{w \left[w^2 + \left(\sqrt{-1.0903} \right)^2 \right]} \quad (3-20)$$

EXAMPLE OF LINVILL'S CONFIGURATION FOR
 REALIZATION OF TRANSFER IMMITTANCE USING
 TWO \overline{RC} CASCADES



ALL VALUES IN OHMS OR FARADS

FIGURE 15

S-PLANE POLE LOCATIONS FOR

$$Z_{21}(s) = \frac{0.056}{\sinh \sqrt{3s} \cosh^3 \sqrt{3s} (\tanh^2 - Q^2)}$$

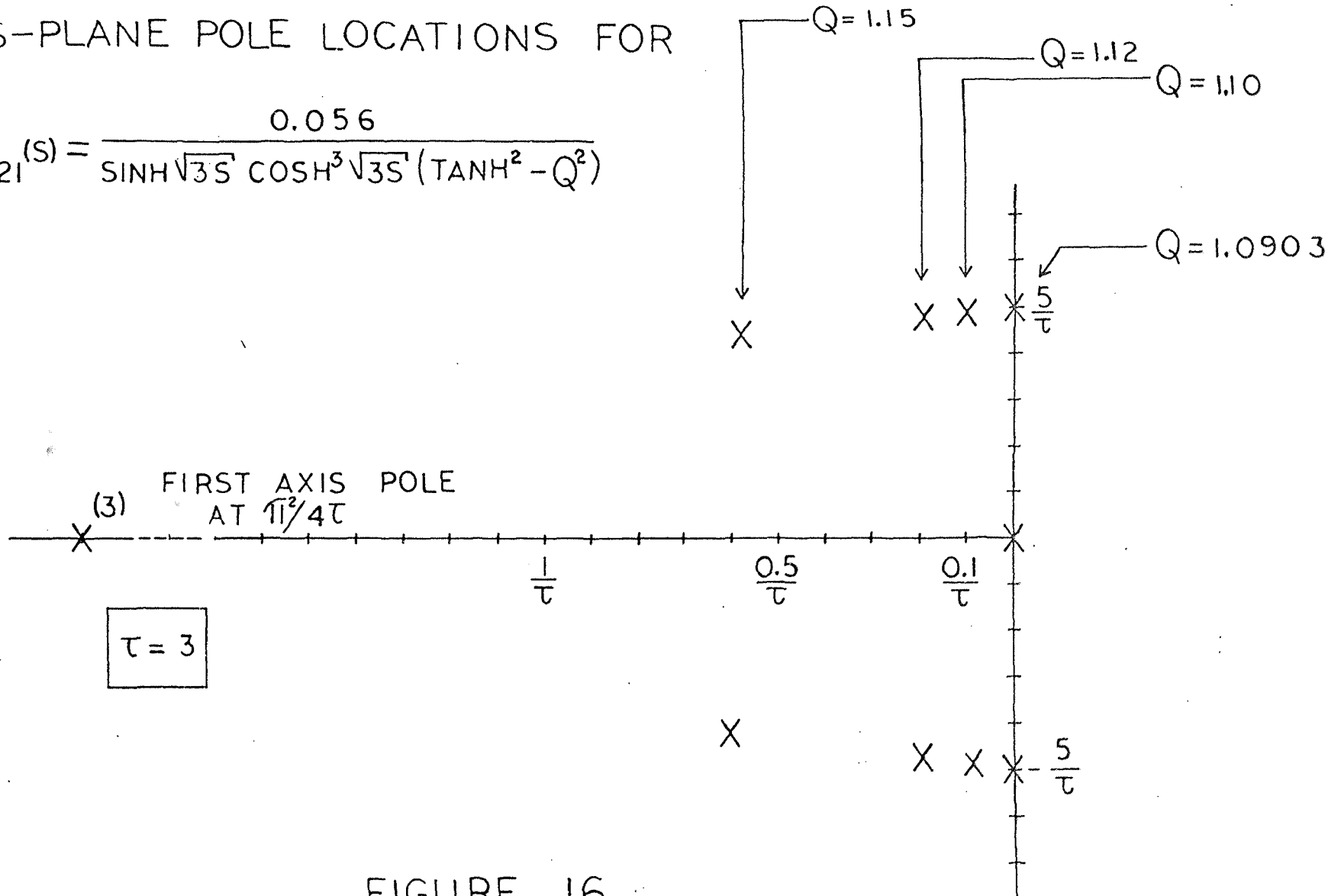


FIGURE 16

The roots of equation (3-20) are located at the following points in the S-plane

$$S = 0, -\frac{\pi^2}{4\tau}, \frac{\pi^2}{\tau}, -\frac{9\pi^2}{4\tau}, \dots$$

and

$$S = \pm j \frac{\pi^2}{2\tau}, \pm j \frac{3\pi^2}{2\tau}, \pm j \frac{5\pi^2}{2\tau}, \dots$$

The root locations are on the imaginary axis since the limiting value of $Q=1.0903$ was used. For the case when the value of Q is greater than 1.0903, the S-plane root pairs become complex as shown in Figure 16.

A computer plot, Figure 17, is obtained by letting $S=j\omega$ and the response is presented in db form. The zero line is used as reference where the transfer function is unity. In actuality however, the value of M in section 3-1 equation (3-9) is not unity but $.056\sqrt{\tau}$ which represents a shift of -20.2 db. The response of the example is plotted over two decades in terms of the normalized units $\frac{\pi^2}{2RC}$.

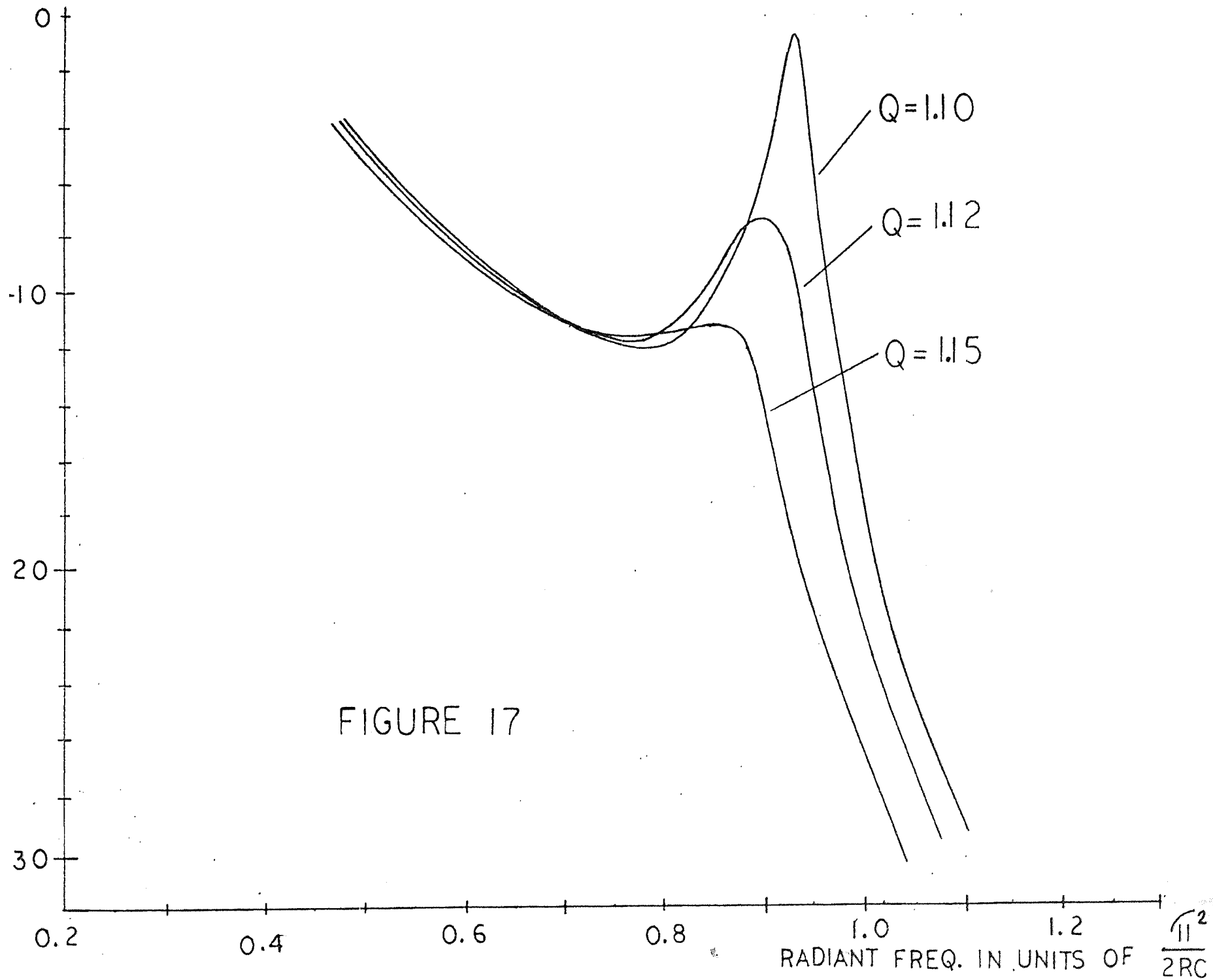


FIGURE 17

CHAPTER IV. CONCLUSION

4-1 Summary of Results

The negative impedance converter in the Linvill configuration is an effective active element in producing complex poles in the transfer function Z_{21T} when the passive networks are \overline{RC} cascades who by themselves do not possess complex S-plane poles.

The pole producing term in the W-plane Z_{21T} function is $(W^2 - Q_1^2)$, which produce LHP poles in the S-plane with the restriction $Q_1 > 1.0903$. For $Q_1 < 1.0903$ the poles are in the RHP and the response becomes unstable.

The transfer impedance generated via the Linvill procedure using only cascaded \overline{RC} elements contains an S-plane pole at the origin. This prevents the synthesis of band-pass filters employing only \overline{RC} cascades without the use of shunt stubs. This limitation of the circuit is not so serious since the voltage transfer ratio for the configuration shown in Figure 13 does not contain any poles at the origin in the S-plane.

4-2 Suggestions for Future Work

Since a variety of network synthesis procedures have been developed, the boundary limitations for realizability and stability are not necessarily included

in the development of such procedures. A similar procedure used in this thesis should be extended to other configurations to determine the limitations of realizability criteria and to identify the boundaries of stability.

An extension of the cascaded RC elements to cascaded and shunt (stubs) RC elements in the Linvill configuration is suggested.

APPENDIX A

8

Consider Wyndrum's positive real transformation

$$S_1(\sqrt{s}) = \tanh \frac{a}{2} \sqrt{s} = \Sigma_1 + j\Omega_1 \quad (1)$$

where the coordinates in the \sqrt{s} plane are $U + jV$.

Using the substitution for \tanh and letting $\sqrt{s} = U + jV$ equation (1) becomes

$$\tanh \frac{a}{2} \sqrt{s} = \frac{\sinh(\frac{a}{2}U + j\frac{a}{2}V)}{\cosh(\frac{a}{2}U + j\frac{a}{2}V)} \quad (2)$$

$$\tanh \frac{a}{2} \sqrt{s} = \frac{\sinh(\sqrt{z}U + j\sqrt{z}V)}{\cosh(\sqrt{z}U + j\sqrt{z}V)} \quad (3)$$

expanding (3) yields,

$$\tanh \sqrt{z}s = \frac{\sin \sqrt{z}U \cosh j\sqrt{z}V + \sinh j\sqrt{z}V \cosh \sqrt{z}U}{\cosh \sqrt{z}U \cosh j\sqrt{z}V + \sinh j\sqrt{z}V \sinh \sqrt{z}U} \quad (4)$$

Substituting $\sinh j\theta = j \sin \theta$ and $\cosh j\theta = \cos \theta$ into (4) and multiplying through by the conjugate of the denominator yields equation (5) after simplification and identification of terms.

$$\tanh \sqrt{z} S' = \frac{\sinh \sqrt{z} U \cosh \sqrt{z} U + j \sin \sqrt{z} V \cos \sqrt{z} V}{\cos^2 \sqrt{z} V + \sinh^2 \sqrt{z} U} \quad (5)$$

The coordinates of the *tanh* plane in terms of the coordinates of the \sqrt{z} plane are given by (6) and (7) below

$$\Sigma_1 = \frac{\sinh \sqrt{z} U \cosh \sqrt{z} U}{\cos^2 \sqrt{z} V + \sinh^2 \sqrt{z} U} \quad (6)$$

$$\Omega_1 = \frac{\sin \sqrt{z} V \cos \sqrt{z} V}{\cos^2 \sqrt{z} V + \sinh^2 \sqrt{z} U} \quad (7)$$

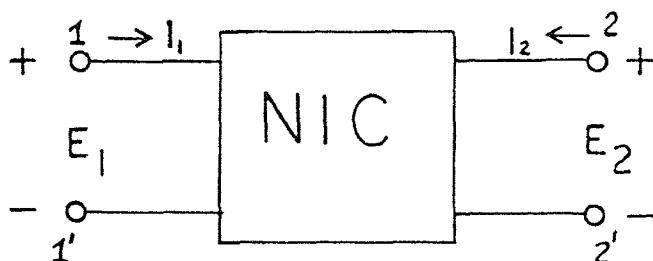
Equations (6) and (7) provide the required transformation from the distributed LC plane to the lumped LC plane.

APPENDIX B

7

The ideal negative-impedance converter is an active two-port device with the property that the driving point impedance or admittance at one terminal pair is the negative of the impedance or admittance connected at the other terminal pair.

The description of the NIC properties are obtained by considering the relationship between the terminal voltages and the currents of the two-port device. Consider the two-port shown below;



where the voltage and current interrelationships are given by the hybrid g parameters

$$\begin{vmatrix} I_1 \\ E_2 \end{vmatrix} = \begin{vmatrix} g_{11} & g_{12} \\ g_{21} & g_{22} \end{vmatrix} \begin{vmatrix} E_1 \\ I_2 \end{vmatrix} \quad (1)$$

The input admittance $\frac{I_1}{E_1}$ at terminals 1-1' is given by

$$\frac{I_1}{E_1} = Y_{IN(1-1')} = g_{11} - \frac{g_{12} g_{21}}{g_{22} + I_L} \quad (2)$$

For an ideal NIC,

$$Y_{IN(1-1')} = - \frac{1}{Z_L} \quad (3)$$

This can only be obtained if

$$g_{11} = 0 \quad (4)$$

$$g_{22} = 0 \quad (5)$$

and

$$g_{12} g_{21} = 1 \quad (6)$$

Inserting these values of the hybrid parameters into equation (1) yields

$$\begin{vmatrix} I_1 \\ E_2 \end{vmatrix} = \begin{vmatrix} 0 & 1 \\ 1 & 0 \end{vmatrix} \begin{vmatrix} E_1 \\ I_2 \end{vmatrix} \quad (7)$$

Since the Linvill configuration consists of elements in cascade, the ABCD parameters are more useful and shall be developed to express the NIC characteristics. Using the transformation given below

$$\begin{vmatrix} A & B \\ C & D \end{vmatrix} = \begin{vmatrix} \frac{1}{g_{21}} & \frac{g_{22}}{g_{21}} \\ \frac{g_{11}}{g_{21}} & \frac{\Delta g}{g_{21}} \end{vmatrix} \quad (8)$$

the ABCD parameters are identically

$$A = \frac{1}{g_{21}} \quad (9-a)$$

$$B = 0 \quad (9-b)$$

$$C = 0 \quad (9-c)$$

$$D = -g_{12} \quad (9-d)$$

There are two types of negative impedance converters, current inversion negative impedance converter INIC and voltage inversion negative impedance converter VNIC. The ABCD parameters for an INIC are given by equation (9), and the ABCD parameters for a VNIC are given below

$$\begin{vmatrix} A & B \\ C & D \end{vmatrix} = \begin{vmatrix} \frac{1}{g_{21}} & 0 \\ 0 & g_{12} \end{vmatrix} \quad (10)$$

In order to standardize on the notation for the NIC with the notation used in the Linvill configuration, the following substitutions shall be made,

$$g_{12} g_{21} = \frac{1}{K_2} \quad (11)$$

$$\frac{1}{g_{21}} = K_1 \quad (12)$$

The generalized ABCD parameters for a NIC using the notation of (11) and (12) are

$$\begin{vmatrix} A & B \\ C & D \end{vmatrix} = \begin{vmatrix} K_1 & 0 \\ 0 & \pm \frac{K_1}{K_2} \end{vmatrix} \quad (13)$$

where the D term may be either positive (VNIC) or negative (INIC).

APPENDIX C

The equation for the transfer impedance using a cascade of two RC sections per network in the Linvill configuration shown in Figure 13 is of the form

$$Z_{21T_{LC}}(W) = \frac{M(1-W^2)^2}{W(W^2 \pm Q_1^2)} \quad (1)$$

where Q_1 is real.

Using the transformation $W = \tanh \sqrt{z} s$ to transform (1) from the lumped LC plane to the distributed LC plane yields

$$Z_{21T_{LC}}(\sqrt{s'}) = \frac{M}{\sinh \sqrt{z} s' \cosh^3 \sqrt{z} s' (\tanh^2 \sqrt{z} s' \pm Q_1^2)} \quad (2)$$

where the roots of $\cosh \sqrt{z} s'$ are

$$\sqrt{s'} = j \frac{(n + \frac{1}{2})\pi}{\sqrt{z}} \quad n = 0, 1, 2, \dots \quad (3)$$

and the roots of $\sinh \sqrt{z} s'$ are

$$\sqrt{s'} = j \frac{n\pi}{\sqrt{z}} \quad n = 0, 1, 2, \dots \quad (4)$$

To evaluate the roots of $\tanh^2 \sqrt{z} s' \pm Q_1^2$, it is observed that two possible root pairs exist,

$$\tanh^2 \sqrt{z} s' + Q_1^2 = 0 \quad (5)$$

and

$$\tanh^2 \sqrt{z} s' - Q_1^2 = 0 \quad (6)$$

Consider the first possible root pairs

$$\tanh^2 \sqrt{\tau s} + Q_1^2 = 0 \quad (7)$$

Equation (7) is composed of the following product terms,

$$(\tanh \sqrt{\tau s} + j Q_1)(\tanh \sqrt{\tau s} - j Q_1) = 0 \quad (8)$$

Consider the roots of the first term of (8)

$$\tanh \sqrt{\tau s} = -j Q_1 \quad (9)$$

using the identity $\tanh \sqrt{\tau s} = \frac{\sinh \sqrt{\tau s}}{\cosh \sqrt{\tau s}}$ equation (9)

becomes

$$\sinh \sqrt{\tau s} = -j Q_1 \cosh \sqrt{\tau s} \quad (10)$$

or

$$e^{\sqrt{\tau s}} - e^{-\sqrt{\tau s}} = j Q_1 \left[e^{\sqrt{\tau s}} + e^{-\sqrt{\tau s}} \right] \quad (11)$$

regrouping terms

$$-(1 + j Q_1) e^{\sqrt{\tau s}} + (1 - j Q_1) e^{-\sqrt{\tau s}} = 0 \quad (12)$$

dividing both sides by $(1 - j Q_1) e^{-\sqrt{\tau s}}$ yields

$$1 = \left(\frac{1 + j Q_1}{1 - j Q_1} \right) e^{2\sqrt{\tau s}} \quad (13)$$

but

$$\left(\frac{1 + j Q_1}{1 - j Q_1} \right) = \left| \frac{1 + j Q_1}{1 - j Q_1} \right| e^{j(\tan^{-1} Q_1 + 2m\pi)} \quad (14-a)$$

$$\left(\frac{1+jQ_1}{1-jQ_1} \right) = e^{(jz\tau\alpha Q_1 + jz m \pi)} \quad (14-b)$$

since Q_1 is real.

Inserting back into (13) yields

$$1 = \left[e^{jz\tau\alpha^{-1}Q_1 + jz m \pi} \right] e^{z\sqrt{z}S} \quad (15)$$

but

$$1 = e^{j2n\pi} \quad (16)$$

therefore

$$2\sqrt{z}S = jz\pi r_1 - jz\tau\alpha^{-1}Q_1 \quad (17)$$

where $r_1 = (n-m)$.

The roots contributed by (17) lie on the imaginary axis in the \sqrt{z} plane due to the absence of a real component. The roots of (9) are given below

$$\sqrt{z} = \frac{j}{2\sqrt{z}} \left[z\pi r_1 - z\tau\alpha^{-1}Q_1 \right] \quad (18)$$

$r_1 = 0, 1, 2, \dots$

Considering the second product term of (8) and solving for the root locations results in:

$$\log_e \left(\frac{jQ_{i-1}}{jQ_{i+1}} \right) = \log_e \left| \frac{jQ_{i-1}}{jQ_{i+1}} \right| + jz m \pi + j\tau\alpha^{-1} \frac{zQ_i}{Q_i z - 1} \quad (19)$$

again as before $\left| \frac{jQ_1 - 1}{jQ_1 + 1} \right| = 1$, resulting in the following roots

$$\sqrt{s} = \frac{j}{2\sqrt{L}} \left[\pi r_2 - 2 \tan^{-1} Q_1 \right] \quad \begin{array}{l} r_2 = 2(m-n) + 1 \\ r_2 = 1, 2, \dots \end{array} \quad (20)$$

Note that equations (17) and (20) are identical.

Now, considering the roots of equation (6), namely

$$\tanh^2 \sqrt{Ls} - Q_2^2 = 0 \quad (21)$$

which can be represented by a product of two terms,

$$(\tanh \sqrt{Ls} - Q_2)(\tanh \sqrt{Ls} + Q_2) = 0 \quad (22)$$

We consider the first term and use the same identity as in (10), therefore

$$\sinh \sqrt{Ls} = Q_2 \cosh \sqrt{Ls} \quad (23)$$

or

$$e^{\sqrt{Ls}} - e^{-\sqrt{Ls}} = Q_2 \left[e^{\sqrt{Ls}} + e^{-\sqrt{Ls}} \right] \quad (24)$$

Regrouping terms and dividing by $(Q_2 + 1)e^{-\sqrt{Ls}}$ yields,

$$1 = \frac{Q_2 - 1}{Q_2 + 1} e^{2\sqrt{Ls}} \quad (25)$$

but

$$\left(\frac{Q_2 - 1}{Q_2 + 1} \right) = e^{\log_e \left(\frac{Q_2 - 1}{Q_2 + 1} \right)} \quad (26)$$

where

$$\log_e \left(\frac{Q_2 - 1}{Q_2 + 1} \right) = \log_e \left| \frac{Q_2 - 1}{Q_2 + 1} \right| + j 2m\pi + j \Phi \quad (27)$$

and $\Phi = 0, \pi$ for $\left(\frac{Q_2 - 1}{Q_2 + 1} \right) \geq 0$
 < 0

Inserting (27) back into (25) yields

$$-1 = \left[e^{\log_e \left| \frac{Q_2 - 1}{Q_2 + 1} \right| + j 2m\pi + j \Phi} \right] e^{z \sqrt{\tau} s} \quad (28)$$

but $-1 = e^{j\pi + j 2n\pi}$ therefore (28) becomes

$$e^{j\pi + j 2n\pi} = \left[e^{\log_e \left| \frac{Q_2 - 1}{Q_2 + 1} \right| + j(2m\pi + \Phi)} \right] e^{z \sqrt{\tau} s} \quad (29)$$

Solving for the roots of the first term of (22) yields

$$\sqrt{s} = \frac{1}{2\sqrt{\tau}} \log_e \left| \frac{Q_2 - 1}{Q_2 + 1} \right| + j \frac{1}{2\sqrt{\tau}} \left[\pi(r_3 + 1) - \Phi \right] \quad (30)$$

$$r_3 = 2(n - m)$$

$$= 0, 1, 2, \dots$$

A similar counterpart for equation (27) is obtained by solving for the roots of the second term of (22), namely

$$\log_e \left(\frac{1 + Q_2}{1 - Q_2} \right) = \log_e \left| \frac{1 + Q_2}{1 - Q_2} \right| + j 2m\pi + j \Phi \quad (31)$$

$$\Phi = k\pi \quad k = 0, 1, 2, \dots$$

and proceeding in a similar fashion as above, the second set of roots for (6) are given below by

$$\sqrt{s} = -\frac{1}{2\sqrt{\tau}} \log_e \left| \frac{1 + Q_2}{1 - Q_2} \right| - j \frac{1}{2\sqrt{\tau}} \left[\pi r_4 + \Phi \right] \quad (32)$$

$$r_4 = 0, 1, 2, \dots$$

BIBLIOGRAPHY

1. J.G. Linvill, "RC Active Filters," Proc. IRE, vol. 42, pp. 555-564, March, 1954.
2. T. Yanagisawa, "RC Active Networks Using Current Inversion Type Negative Impedance Converters," IRE Trans. on Circuit Theory, vol. CT-4, pp. 140-144, September 1957.
3. J.M. Sipress, "Synthesis of Active RC Networks," IRE Trans. on Circuit Theory, vol CT-9, pp.206-269, September, 1961.
4. I.W. Sandberg, "Active RC Networks," Research Report R662-58, PIB-590, Polytechnic Inst. of Brooklyn, N.Y., May, 1958.
5. B.K. Kinarawala, "Synthesis of Active RC Networks," Bell System Tech. Journal, vol. 38, pp. 1269-1317, September 1959.
6. I.M. Horowitz, "Active RC Transfer Function Synthesis by Means of Cascaded RC and RL Structures," Microwave Res. Inst., Polytechnic Inst. of Brooklyn, N.Y., Report No. R-507-56, pp. 113-437, 1956.
7. A.I. Larky, "Negative Impedance Converters," IRE Trans. Circuit Theory, vol. 4, pp. 124-131, September, 1957.
8. R.W. Wvndrum Jr., "The Exact Synthesis of Distributed RC Networks," Tech. Report 400-76, Dept. Electrical Engineering, New York Univ., May, 1963.
9. R.P. O'Shea, "Synthesis Using Distributed RC Networks," IEEE Internat. Convention Record, part 7, pp. 18-29 , 1965.
10. E.A. Guillemin, "Synthesis of Passive Networks," John Wiley and Sons, Inc., New York, 1957.
11. N. Balabanian, "Network Synthesis," Prentice Hall, Inc., 1958.
12. P.M. Chirlian, "Integrated and Active Network Analysis and Synthesis," Prentice Hall, Inc., 1967.
13. D.A. Calahan, "Modern Network Synthesis," Hayden Book Co., Inc., New York, 1964.

14. P.I. Richards, "Resistor Transmission Line Circuits," Proc. IRE, vol. 30 No. 2, pp. 217-220, February, 1948.
15. J.O. Scanlan and J.D. Rhodes, "Realizability and Synthesis of a Restricted Class of Distributed RC Networks," IEEE Trans. Circuit Theory, vol. 12, pp. 577-585, December, 1965.
16. J. Stein, S. Shamis, and J. Mulligan, "Realization of Transfer Functions Using Uniform RC Distributed Networks with Common Ground Connections," Tech. Report 400-140, Dept. of Electrical Engineering, New York University, June 1966.